ISTANBUL TECHNICAL UNIVERSITY ★ GRADUATE SCHOOL

DESIGN OF AN OPAMP-RC LOWPASS FILTER IN 22 NM FDSOI TECHNOLOGY

M.Sc. THESIS

Ömer Taha KELEŞ

Department of Electronics and Communication Engineering

Electronics Engineering Programme

JUNE 2022

ISTANBUL TECHNICAL UNIVERSITY ★ GRADUATE SCHOOL

DESIGN OF AN OPAMP-RC LOWPASS FILTER IN 22 NM FDSOI TECHNOLOGY

M.Sc. THESIS

Ömer Taha KELEŞ
(504201201)

Department of Electronics and Communication Engineering

Electronics Engineering Programme

Thesis Advisor: Assoc. Prof. Dr. Metin YAZGI

JUNE 2022

ISTANBUL TEKNİK ÜNİVERSİTESİ ★ LİSANSÜSTÜ EĞİTİM ENSTİTÜSÜ

22 NM FDSOI TEKNOLOJİSİNDE OPAMP-RC ALÇAK GEÇİREN FİLTRE TASARIMI

YÜKSEK LİSANS TEZİ

Ömer Taha KELEŞ
(504201201)

Elektronik ve Haberleşme Mühendisliği Anabilim Dalı

Elektronik Mühendisliği Programı

Tez Danışmanı: Doç. Dr. Metin YAZGI

JUNE 2022

Ömer Taha KELEŞ, a M.Sc. student of İTU Graduate School 504201201, successfully defended the thesis/dissertation entitled "DESIGN OF AN OPAMP-RC LOWPASS FILTER IN 22 NM FDSOI TECHNOLOGY", which he/she prepared after fulfilling the requirements specified in the associated legislations, before the jury whose signatures are below.

Thesis Advisor :	**Assoc. Prof. Dr. Metin YAZGI** Istanbul Technical University	.....
Jury Members :	**Assoc. Prof. Dr. Tufan Coşkun KARALAR** Istanbul Technical University	.....
	Assis. Prof. Dr. Okan Zafer BATUR Istanbul Bilgi University	.....

Date of Submission : 08 June 2022
Date of Defense : 02 June 2022

To Sekiro,

FOREWORD

First of all, I would like to express my gratitude to my supervisor Assoc. Prof. Metin Yazgı for his support and understanding.

I would also like to thank to MKR-IC, the company where I work, for every bit of support.

I would like to thank my colleague Hasip Terlemez for his friendship and guidance.

Finally, I would like to thank my family for always being there to support me in every step of my life. My gratitude to them is infinite and endless.

June 2022

Ömer Taha KELEŞ
Engineer

TABLE OF CONTENTS

Page

ABBREVIATIONS

AC	**:** Alternative Current
ADC	**:** Analog to Digital Converter
BOX	**:** Buried Oxide
CMFB	**:** Common Mode Feedback
CMOS	**:** Complementary Metal Oxide Semiconductor
DC	**:** Direct Current
DPD	**:** Digital Pre-Distortion
ENOB	**:** Effective Number of Bits
FDSOI	**:** Fully Depleted Silicon on Insulator
MIMO	**:** Multiple Input Multiple Output
MOM	**:** Metal-on-Metal
MOSFET	**:** Metal Oxide Semiconductor Field Effect Transistor
NMOS	**:** N-Channel Metal Oxide Semiconductor Field Effect Transistor
OTA	**:** Operational Transconductance Amplifier
PMOS	**:** P-Channel Metal Oxide Semiconductor Field Effect Transistor
RDF	**:** Random Dopant Fluctuation
RF	**:** Radio Frequency
RX	**:** Receiver
SFDR	**:** Spurious Free Dynamic Range
SoC	**:** System on Chip
SPI	**:** Serial Peripheral Interface
THD	**:** Total Harmonic Distortion

SYMBOLS

C	**:** Capacitance
R	**:** Resistance
L	**:** Inductance
g_m	**:** Transconductance Gain
dB	**:** Decibel
dBc	**:** Decibels Relative to the Carrier
°	**:** Degree

LIST OF TABLES

Page

LIST OF FIGURES

Page

DESIGN OF AN OPAMP-RC LOWPASS FILTERIN 22 NM FDSOI TECHNOLOGY

SUMMARY

Analog filters are widely used in signal processing applications like noise reduction, blocker rejection, signal detection, anti-aliasing, demodulation, audio processing etc. They are utilized to allow certain signals to pass while blocking others. Passed or blocked signals are not time dependent since analog filters are time invariant circuits. These filters pass or block signals depending on the signal's frequency, meaning that signals in specified frequency ranges are blocked or passed. While time domain responses of the filters are still a critical design consideration, filters are mainly designed considering the desired frequency domain responses. Main types of filters can be categorized as lowpass, highpass, bandpass and bandstop according to their selective frequency range.

There are various types of lowpass filter responses which have different passband or stopband characteristics. Brick wall response, whose pass and stop bands are separated at the corner frequency, has a discontinuous frequency response. This type of a mathematical function is not realizable in real world. On the other hand, realizable filter responses are continuous functions with finite roll-off slopes between stopband and passband. The slope at the transition band depends on the order of the filter function and the type of the filter function. Additionally in real filter functions there may be permitted fluctuations which may appear in stopband, passband or both. In Butterworth response, the passband has flat frequency characteristics so it is called maximally flat magnitude response. Likewise, Chebyshev type I filter response has equal ripples in the passband so it is called equal ripple magnitude response. Chebyshev type II filter response, or equal ripple stopband magnitude response, has equal ripples in the stopband and Cauer filters have ripples in both stopband and passband.

The question of how to realize filter functions with real circuit elements arises numerous solutions. Such filter functions can be realized using circuit elements like resistors, capacitors, inductors and some specialized circuit elements such as operational amplifiers and switched capacitors. Filter characteristics and design limitations vary greatly depending on the circuit elements and topologies used. In order to realize lowpass filter functions, various different circuit topologies are proposed over the last couple of decades. Filters are classified depending on the circuit elements employed. LC ladder filters consist of inductors, capacitors and resistors which are all passive elements. Besides resistors and capacitors, Opamp-RC filters utilize active circuit elements called operational amplifiers. Moreover, OTA-C filters are implemented using operational transconductance amplifiers and capacitors. Furthermore, capacitors, operational amplifiers and switched capacitor circuits are used to build switched capacitor filters. All the different circuit topologies have their advantages and disadvantages. It is the designer's job to determine which topology is a better choice considering the design specifications and limitations.

Over the years, shrinking of transistor sizes resulted in reduced analog performance and lower voltage headroom. For this reason, several process techniques have been developed. One of them is fully depleted silicon on insulator (FDSOI) technology. FDSOI technology provide less process variation and leakage current compared to the similar channel length bulk CMOS processes. For this reason, FDSOI is considered as an alternative to the further reduced silicon geometries. The channel is electrically isolated from the transistor bulk by a thin layer of buried oxide. This isolation results that the amount of leakage current is reduced and parasitic diode effects are lessened. Also, since the channel is undoped, transistors are more prone to process variations.

With these considerations, an opamp-RC lowpass filter is designed in 22 nm FDSOI technology to comply with the design requirements. The designed filter consists of a 3rd order Chebyshev type I lowpass filter and a first order filter with variable gain. A Tow-Thomas biquad following a first order RC filter is used in the 3rd order filter. A high gain-bandwidth operational amplifier is designed to be used in both Tow-Thomas biquad and variable gain first order filter. Power supply is 0.8 V and total power consumption is 7.6 mW for the filter circuit. Less than 1dB attenuation or ripple up to 25 MHz and more than 60 dB attenuation after 240 MHz is obtained. Also 81 dB SFDR and 7.6 bits ENOB values are achieved for full scale input and 800 mV peak-to-peak output swing.

TÜRKÇE TEZ BAŞLIĞI BURAYA YAZILIR

ÖZET

Analog filtreler sinyal işleme uygulamalarında kullanılan temel bloklardan biridir. Gürültü bastırma, blokör engelleme, sinyal tespiti, örtüşme önleme, demodülasyon ve ses işleme bu uygulamalardan birkaçı olarak gösterilebilir. Geçmişte özellikle telekomünikasyon teknolojilerinin gelişmesinde analog filtreler kritik rol oynamıştır. Günümüzde ise filtreleme işlemlerinin bir kısmı dijital alana kaymış olsa da yüksek frekanslı veya alt dereceli filtreleme işlemleri için analog filtreler dijital filtrelere kıyasla daha uygulanabilir ve daha düşük maliyetli kalmaktadır.

Analog filtreler belirli sinyallerin geçmesine izin verirken belirli sinyallerin de geçmesini engellemek için kullanılan devre elemanlarıdır. Filtrelerin sinyalleri geçirmesi veya bloklaması bu sinyallerin bulunduğu frekans bandına bağlıdır. Bu da demektir ki belirli frekans aralığındaki sinyaller filtre tarafından geçirilirken belirli frekans aralığındaki sinyaller de filtre tarafından bloklanmaktadır. Filtreleri zaman alanındaki cevapları her ne kadar kritik olmaya devam etse de filtrelerin karakterizasyonu asıl olarak frekans alanında yapılmaktadır. Başlıca filtre cevapları alçak geçiren filtre, yüksek geçiren filtre, bant geçiren filtre ve bant durduran filtre olarak kategorize edilebilir. Bu karakterizasyon filtrenin geçirdiği veya blokladığı sinyallerin frekans aralığına göre yapılmaktadır.

Alçak geçiren filtrelerin gerçeklenmesinde baz alınan birkaç farklı frekans cevabı çeşidi vardır. İdeal filtre cevabının geçirme ve bloklama bantları köşe frekansında ayrılmıştır. Bu ayrım süreksiz bir filtre cevabı demektir. Bu şekildeki süreksiz bir filtre cevabının gerçek dünyada bir karşılığı ve uygulanabilirliği yoktur. Buna karşın belirli bazı sürekli frekans cevapları gerçeklenebilir ki bu frekans cevaplarında geçirme ve bloklama bandı arasındaki bir transisyon bandında eğim sonludur. Buna ek olarak filtre fonksiyonlarında geçirme bandında, bloklama bandında veya her ikisinde yüksekliği belli dalgalanmalara izin verilebilir. Bu durum göz önüne alındığında farklı filtre cevapları elde edilir. Butterworth filtre cevabında geçirme bandı düzdür ve bu cevaba aynı zamanda azami ölçüde düz geçirme bandı cevabı da denir. Chebyshev tip I filtre cevabında ise geçirme bandı içerisinde yüksekliği belli olan dalgalanmalar vardır ve bu filtre cevabına aynı zamanda eşit genlik dalgalanmalı geçirme bandı cevabı da denir. Benzer şekilde Chebyshev tip II filtre cevabı, ya da eşit genlik dalgalanmalı bloklama bandı cevabı, bloklama bandında eşit genlikli dalgalanmalar barındırır. Cauer filtre cevabında ise hem geçirme bandında hem de bloklama bandında dalgalanmalar vardır.

Filtre cevaplarının nasıl gerçeklenebileceği sorusunun birden fazla cevabı vardır. Filtre cevabı çeşitleri direnç, kapasitör, endüktör gibi pasif devre elemanları veya operasyonel yükselteç, anatarlanan kapasitör gibi aktif devre elemanları kullanılarak gerçeklenebilir. Filtrelerin karakteristik özellikleri, tasarım ölçütleri ve kısıtlamaları devrede kullanılan elemanlara ve devrenin topolojisine önemli ölçüde bağlıdır. Alçak geçiren filtrelerin gerçeklenebilmesi için son birkaç on yıl içerisinde çeşitli devre

topolojileri önerilmiştir. Başlıca filtre topolojileri farklı başlıklar altında toplanabilir. LC merdiven filtrelerde dirençler, endüktörler ve kapasitörler kullanılır. Bu da demektir ki LC merdiven filtrelerde sadece pasif elemanlar kullanılmaktadır. Bu sebeple bu filtrelerden kazanç sağlamak mümkün olmamaktadır. Ayrıca günümüz teknolojilerinde transistör boyutları oldukça küçülmüşken endüktör boyutları transistörlere kıyasla çok büyük olmaktadır. Bu da kısıtlı tasarım alanı olan tasarımlarda büyük sorun teşkil etmektedir. Opamp-RC filtrelerde direnç ve kapasitörlere ek olarak operasyonel yükselteçler de kullanılır. Operasyonel yükselteçler aktif elemanlar olup güç harcamaktadır. Opamp-RC filtreler kullanılarak birinci ve ikinci dereceden filtre fonksiyonları gerçeklenebilir. Bu da demek olur ki daha yüksek dereceden filtre fonksiyonları da opamp-RC filtreler aracılığıyla gerçeklenebilir çünkü ikinci dereceden daha yüksek olan filtre fonksiyonları birçok ikinci dereceden ve eğer filtre fonksiyonu derecesi tek ise ek olarak bir birinci dereceden fonksiyonun çarpımı olarak ayrıştırılabilir. Böylece ikinci dereceden filtreler ve eğer filtre derecesi tek ise ek olarak birinci dereceden bir filtre arka arkaya bağlanarak daha yüksek dereceli filtreler elde edilebilir. Opamp-RC filtreler lineerliği yüksek olması sebebiyle sıklıkla tercih edilmektedir. OTA-C devrelerde ise kapasitörler ve operasyonel transkondüktans yükselteçler kullanılır. Bu filtrelerde LC merdiven filtrelerde kullanılan endüktörler ve dirençler terine transkondüktör yükselteçleriyle birlikte kapasitörler kullanılarak aynı filtre fonksiyonları gerçeklenebilir. Böylece endüktörlerin kapladığı aşırı serim alanına gerek kalmadan aynı fonksiyonlar gerçeklenmiş olur. Ayrıca transkondüktör yükselteçlerin transkondüktans değerleri kalibre edilerek filtre fonksiyonunu oluşturan elemanların değerlerini kalibre etmek mümkün olmaktadır. Anahtarlanabilir kapasitör filtrelerde ise kapasitörlere ve operasyonel yükselteçlere ek olarak topolojinin isminden de anlaşılabileceği üzere anahtarlanabilir kapasitörler kullanılır. Bu filtrelerde direnç elemanı yerine anahtarlanabilir kapasitörler kullanılmaktadır. Böylece üretim sürecinde varyasyonlar gösteren dirençler yerine anahtarlanabilir kapasitörler kullanılmış olur. Tüm bu farklı filtre topolojileri kendilerine ait avantajlara ve dezavantajlara sahiptir. Bu avantajları, dezavantajları ve tasarım spesifikasyonlarını göz önünde bulundurarak tasarlanacak filtrenin topolojisini seçmek filtre tasarımcısının görevlerinden biridir.

Filtrelerin tasarlanma amaçlarına göre veya kullanıldıkları sisteme ve etkileşime geçtikleri bloklara bağlı olarak sağlamaları gereken belirli spesifikasyonlar vardır. Bu spesifikasyonlar frekans alanında olabileceği gibi zaman alanında da olabilir. Geçiş bandının sınırı geçiş bandı köşe frekans olarak adlandırılırken bloklama bandının sınırı ise bloklama bandı köşe frekansı olarak adlandırılır. Bu frekanslar ve bloklama bandında sağlanması gereken sönümleme değeri filtre tasarımında kritik önem taşır. Buna ek olarak filtre tasarımı geçirme bandındaki ve bloklama bandındaki dalgalanma değerleri belirli sınırlar içerisinde kalacak şekilde yapılmaktadır. Frekans alanındaki spesifikasyonlara ek olarak zaman alanında da spesifikasyonlar bulunmaktadır. Filtrelerin işledikleri sinyallere ekledikleri gürültü ve işledikleri sinyallerin lineerliğinde yol açtıkları bozulmalar da göz önüne alınmaktadır. Bu parametreler tasarlanacak filtrenin frekans cevabı çeşidinin seçilmesinde ve filtre topolojisinin seçiminde rol oynar.

Yıllar içerisinde transistör boyutlarındaki küçülme analog performansta düşüşü ve voltaj payındaki düşüşü de beraberinde getirmiştir. Bundan dolayı CMOS gövde teknolojisine alternatif yeni teknolojiler geliştirilmiştir. Bu teknolojilerden biri de FDSOI teknolojisidir. FDSOI teknolojisinde gömülü oksit katmanı transistör kanalını

gövdeden izole eder. Bu izolasyonun sonucu olarak FDSOI teknolojisindeki transistörlerde CMOS gövde teknolojisindeki transistörlere kıyasla kaçak akım miktarı azdır, üretim sürecindeki performans varyasyonları daha azdır. Bu sebeple FDSOI teknolojisi düşük kanal genişlikli CMOS gövde teknolojisine bir alternatif olarak görünmektedir. FDSOI teknolojisinin getirdiği en önemli avantajlardan biri de her transistörün gövde geriliminin bağımsız şekilde ayarlanabilir olmasıdır. Transistörlerin kanalları gövdeden gömülü oksit tabakasıyla ayrıldığı için farklı transistörlerin kanalları arasında izolasyon sağlanmış olmaktadır. Bu izolasyon gövde gerilimi değerinin ayarlanması açısından serbestlik tanımaktadır. Bu sebeple eşik gerilimini kaydırma amacıyla gövde gerilimini değiştirmek mümkün olmaktadır. Buna ek olarak transistörü gövdeden sürebilmek de daha kolaylaşmaktadır. Kanalın gövdeden izole olmasının önünü açtığı uygulamalardan biri de NMOS transistörlerin PWELL kuyuları yerine NWELL kuyularına gerçeklenebilmesidir. Böylece NMOS gövde gerilimleri kaynak gerilimine kadar yükseltilebilmektedir ve eşik gerilimleri bu şekilde aşağı çekilmektedir. Aynı şekilde kanalın gövdeden izole olması PWELL transistörlerin NWELL kuyuları yerine PWELL kuyularına gerçeklenmesine olanak sağlamaktadır. Böylece PMOS transistörlerin gövde gerilimleri toprak gerilimine bağlanarak eşik geriliminde azaltma sağlanabilir. Bu tasarım esnekliği voltaj aralığı düşük olan tasarım teknolojilerinde kritik önem taşımaktadır. NMOS transistörlerin NWELL kuyularına ve PMOS transistörlerin de PWELL kuyularına gerçeklenmesi tersyüz kuyu konfigürasyonu olarak isimlendirilmektedir.

Bunlar göz önünde bulundurularak, belirli spesifikasyonları sağlamak üzere 22 nm FDSOI teknolojisinde bir opamp-RC alçak geçiren filtre tasarlanmıştır. Tasarlanan filtre dördüncü dereceden olup üçüncü dereceden bir Chebyshev tip I alçak geçiren filtreden ve birinci dereceden ayarlanabilir kazançlı alçak geçiren filtreden oluşmaktadır. Üçüncü dereceden filtreyi bir birinci dereceden RC filtreyi takip eden Tow-Thomas devresi oluşturur. Hem Tow-Thomas devresinde hem de birinci dereceden ayarlanabilir kazançlı alçak geçiren filtrede kullanılmak üzere yüksek kazanç bant genişlikli bir operasyonel yükselteç tasarlanmıştır. Filtre 0.8 voltluk gerilimde 22 nm FDSOI teknolojisinde tasarlanmıştır. Toplam güç tüketimi 7.6 mW civarındadır. 25 MHz frekansına kadar maksimum 1dB dalgalanma veya sönümleme, 240 MHz frekansı sonrasında ise en az 60 dB sönümleme sağlanmıştır. Ayrıca 81 dB SFDR ve 7.6 bit ENOB değerleri tepeden tepeye 800 mV çıkış genliği için sağlanmaktadır.

Bu tez kapsamında analog filtrele cevaplarının çeşitleri, filtrelerin gerçeklenmesi için kullanılan temel topolojileri, filtrelerin performans metrikleri ile alakalı temel bilgilere yer verilmiştir. Ardından FDSOI teknolojisinden ve bu teknolojinin gövde CMOS teknolojisine kıyasla sağladığı avantajlardan bahsedilmiştir. Son olarak da belirli spesifikasyonları sağlamak üzere tasarlanan filtrenin yapısı ve simülasyon sonuçlarına yer verilmiştir.

1. INTRODUCTION

In signal processing, analog filters are considered as essential building blocks particularly in the telecommunication applications [1], [2]. Analog filters have played a critical role in a variety of technological breakthroughs and provided telecommunication companies with substantial profits. Early developments in transmission line applications gave rise to the electronic filter theory since the electronic filters were first and mainly used in transmission lines in telecommunication applications. The introduction of network synthesis techniques, on the other hand, considerably increased the designer's level of control on the design parameters. So that engineers were capable of realizing more complex mathematical filter functions with more precision. While for many filtering applications digital filters are used with the development of integrated circuitry, analog filters still essential for applications such as frequency duplexing, power amplifier impedance matching, suppression in conversion mixers, anti-aliasing in data converters [3].

With the consideration of the applications and demands, different types of filter topologies are developed. Firstly, as a result of the advancement in the transmission line theory, passive filter topologies like LC ladder filters are constructed. In the recent decades with the improvements on the network synthesis techniques, active filters such as OTA-C, opamp-RC, switched capacitor filters are developed. Compared to the earlier developed passive filters like LC ladder filters, active filter topologies provide more reliability and easier implementation with reduced complexity.

Opamp-RC filters are one of the commonly used active filter topologies. This type of filters include operational amplifier circuits in addition to resistors and capacitors. Closed loop nature of the opamp-RC topology results that these filters achieve exceptional linearity [4], [5] in addition to low noise performance and large voltage swing [6] while the performance of an opamp-RC filter heavily depends on the operational amplifier’s gain-bandwidth product, gain and output impedance. Multistage operational amplifiers are commonly used for opamp-RC filter applications

since they can achieve high gain and gain-bandwidth product, with large voltage swing at the output.

Shrinking transistor sizes has resulted in development of new processes alternative to the bulk CMOS process because of the reduced analog performance and low voltage headroom. Fully depleted silicon on insulator (FDSOI) technology is considered one of the alternatives to the further shrunk bulk CMOS processes. FDSOI MOSFETs provide improvement in process variation, leakage current and analog performance compared to the bulk CMOS counterparts [7], [8], [9]. For this reason, FDSOI is considered as an alternative to the further reduced silicon technologies. FDSOI MOSFETs also provide design flexibilities such as independent back gate biasing and flip-well configuration.

While designing an analog filter, firstly a mathematical filter response is selected or constructed considering the requirements and specifications. There are well known filter functions such as Butterworth response, Chebyshev response etc. After determining the filter response and filter order, a filter topology is selected as which the filter will be implemented. Design of additional peripheral blocks may be required to calibrate the frequency response of the filter or output DC offset voltage.

1.1 Purpose of Thesis

In this thesis, lowpass filter responses and filter implementation circuit topologies are examined. Additionally, FDSOI process technology and its advantages over bulk CMOS processes are mentioned. Finally design of an opamp-RC lowpass filter circuit in 22 nm FDSOI technology is explained and simulation results are presented.

1.2 Organization of the Thesis

This thesis consists of 4 chapters.

In the first chapter a brief introduction is given. Purpose and organization of the thesis are presented.

In chapter 2, an overview of analog lowpass filters responses, lowpass filter circuit topologies and filter performance parameters are given. Additionally, an overview of FDSOI technology is presented.

In chapter 3, the design of the opamp-RC lowpass filter is explained in detail. Also, simulation results of the designed filter are presented. Finally, layouts of the filter and opamp circuits are given.

In chapter 4, the thesis is concluded.

2. OVERVIEW

In this chapter, fundamental information about analog filters is given. After that, common methods of analog filter implementation are mentioned including certain topologies. Then design and performance metrics for analog filters are briefly explained. Finally, FDSOI process technology and its benefits are addressed.

2.1 Analog Filter Fundamentals

Analog filters, or continuous time filters, are essential to variety of electrical engineering applications. A few of these applications are, noise reduction, blocker rejection, signal detection, demodulation, audio processing, etc. Analog filters are used simply to pass certain signals and attenuate others. Analog filters are time invariant circuits so passed or attenuated signals are not time dependent. These filters are designed to pass or attenuate signals in particular frequencies. This means that analog filters are analyzed and designed mainly considering frequency domain while transient responses of the filters are still a critical aspect of the design. Analog filters are realized using resistors, capacitors, inductors and some specialized circuit elements such as operational amplifiers. Depending on the circuit elements used, filter characteristics vary greatly as will be explain in following chapters.

An analog filter can be modelled as a two-port device as in Figure 2.1 below.

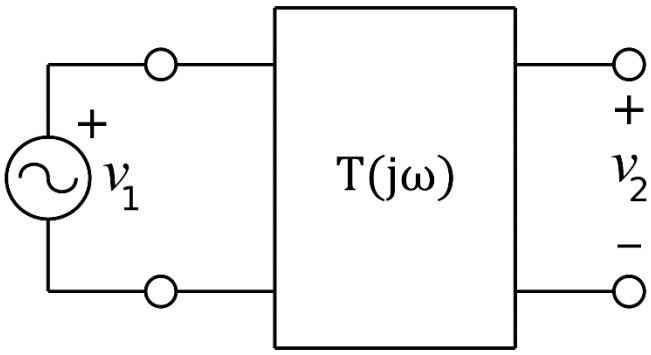

Figure 2.1 : Two-port model of an analog filter.

When input and output quantities are expressed by their Laplace transforms, the filter's transfer function can be defined as

$$\frac{V_2}{V_1} = T(s) = |T(j\omega)|\, e^{j\theta(\omega)}, \qquad \frac{|V_2|}{|V_1|} = |T(s)| \tag{2.1}$$

Transfer function of a filter indicates how much attenuation does the filter have and how much phase shift is created by the filter at any given frequency. Magnitude of the transfer function is commonly expressed in dB as the following equation where α is a measure of attenuation (or gain when negative sign is removed).

$$\alpha(\omega) = -20\log|T(j\omega)|\, dB \tag{2.2}$$

Depending on the frequency range of pass and stop bands, filters are categorized as follows:

- Lowpass filter has a characteristic where passband extends from zero frequency to a frequency called cutoff frequency (or passband corner frequency) denoted as ω_C (or f_C).
- Highpass filter stopband extends from the corner frequency ω_C to infinity while signals that has frequency between zero and ω_C are stopped. Highpass filter characteristic is complementary to lowpass filter.
- Bandpass filter has a passband ranging from ω_1 to ω_2, while signals out of this band are stopped.
- Bandstop filter characteristic is complementary to the bandpass filter. Signals with frequency between ω_1 and ω_2 are stopped while signals at other frequencies are passed. This filter type also referred as notch filter.

Magnitude responses as a function of frequency for four filter types can be seen in the Figure 2.2. Dark blue solid lines represent ideal filter functions and red dashed lines represent realistic filter functions.

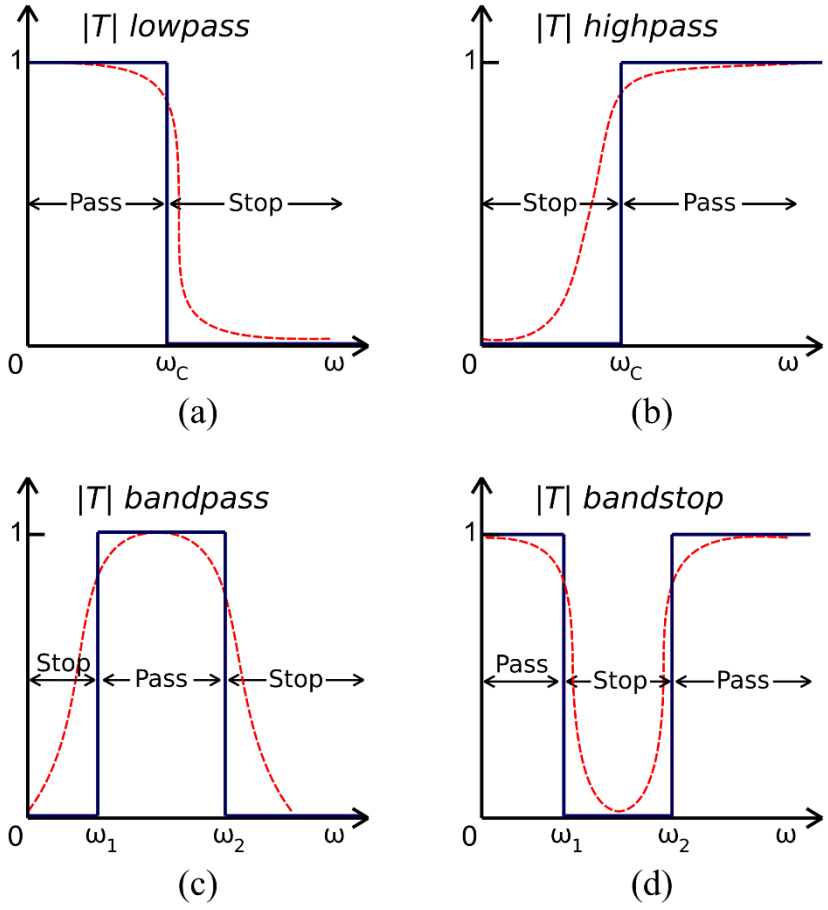

Figure 2.2 : Magnitude responses as functions of frequency for a) lowpass, b) highpass, c) bandpass and d) bandstop filter functions.

2.2 Types of Lowpass Filter Responses

For the ideal lowpass filter characteristic, stopband and passband are distinctly separated at the cutoff frequency. However, this brick wall response is not realizable. Real filter responses can only have finite slope roll-off between passband and stopband which means there is a transition band between. The sharpness of this roll-off depends on the filter order. If the filter order is higher, a sharper transition will occur, so it will be closer to the ideal filter response. In addition to the roll-off characteristic, real filters exhibit fluctuations in stopband, passband or both. These fluctuations are called ripples. When all considered, different types of filter responses vary greatly. Most commonly used types of these responses are mentioned in following chapters.

2.2.1 Butterworth filters (maximally-flat magnitude response)

Butterworth response is a filter response type that have flat passband response meaning that there are no ripples at the passband.

The filter transfer function $T(j\omega)$ which is a complex function can be written as

$$T(j\omega) = Re\,T(j\omega) + j\,Im\,T(j\omega) \tag{2.3}$$

Knowing that Re is an even and Im is an odd function, following is also true

$$T(-j\omega) = ReT(j\omega) - j\,Im\,T(j\omega) \tag{2.4}$$

which means

$$T(-j\omega) = T^*(j\omega) \tag{2.5}$$

Since

$$T(-j\omega)\,T^*(j\omega) = (Re\,T(j\omega))^2 + (Im\,T(j\omega))^2 = |T(j\omega)|^2 \tag{2.6}$$

following equation is also correct

$$|T(j\omega)|^2 = T(j\omega)\,T(-j\omega) \tag{2.7}$$

It is clear that this is also an even function, meaning that

$$|T(j\omega)|^2 = |T(-j\omega)|^2 \tag{2.8}$$

At this point let's write the function as a division of a numerator and denominator polynomials which will must be even functions, and n representing the degree of the polynomials

$$|T_n(j\omega)|^2 = \frac{|N_n(j\omega)|^2}{|D_n(j\omega)|^2} = \frac{X(\omega^2)}{Y(\omega^2)} \tag{2.9}$$

noting that ω is the normalized frequency. Now it is handy to define a function $K(j\omega)$ which is the deviation of the $T_n(j\omega)$ transfer function from unity as

$$|K(j\omega)|^2 = |T_n(j\omega)|^{-2} - 1 = \frac{Y(\omega^2)}{X(\omega^2)} - 1 = \frac{Y(\omega^2) - X(\omega^2)}{X(\omega^2)} \tag{2.10}$$

For a lowpass filter it is obvious that it would require that $|K(j\omega)|$ is close to zero at lower frequencies and it is much higher in upper frequencies. Simplifying the equations (2.9) and (2.10) by choosing

$$X(\omega^2) = 1 \tag{2.11}$$

Means that the function will not have any zeros in finite frequencies. The simplified equations are as follows

$$|T_n(j\omega)|^2 = \frac{1}{1 + Y_2\omega^2 + Y_4\omega^4 + \ldots + Y_{2n}\omega^{2n}} \tag{2.12}$$

$$|K(j\omega)|^2 = Y_2\omega^2 + Y_4\omega^4 + \ldots + Y_{2n}\omega^{2n} \tag{2.13}$$

In order to have the flattest possible response in passband, at zero frequency derivatives of the $|K(j\omega)|^2$ should be zero. This possible when coefficients of the $|K(j\omega)|^2$ polynomial are zero (except for Y_{2n}, otherwise transfer function would be equal to zero) as shown in

$$\left.\frac{d^m(|K(j\omega)|^2)}{d(\omega^2)^m}\right|_{\omega=0} = 0, \qquad for\ m = 1,2,3,\ldots,n-1 \tag{2.14}$$

$$Y_2 = Y_4 = \ldots = Y_{2(n-1)} = 0 \tag{2.15}$$

Y_{2n} can be replaced with ε^2 as, creating the expression

$$|K(j\omega)|^2 = Y_{2n}\omega^{2n} = \varepsilon^2\omega^{2n} \tag{2.16}$$

and

$$|T_n(j\omega)|^2 = \frac{1}{1 + Y_{2n}\omega^{2n}} = \frac{1}{1 + \varepsilon^2\omega^{2n}} \tag{2.17}$$

When ε^2 chosen to be 1, the new transfer function is called Butterworth response:

$$|T_n(j\omega)|^2 = \frac{1}{1 + \omega^{2n}} \tag{2.18}$$

From the equation (2.18) it can be seen that at the $\omega = 1$ frequency, attenuation is 3dB independent of the function degree. Also, for large values of ω attenuation slope is n×20dB per decade. In the Figure 2.3, Butterworth magnitude responses for filters with orders 2 to 10 can be seen.

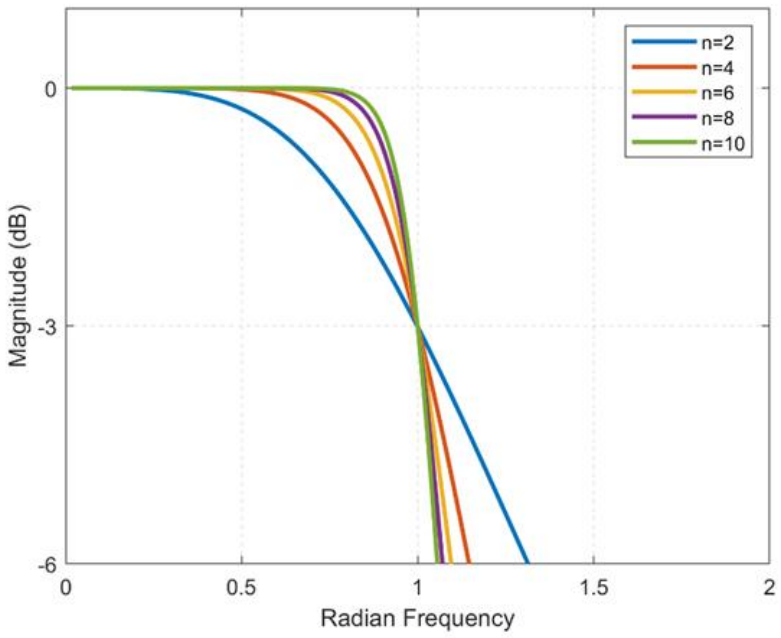

Figure 2.3 : Butterworth magnitude responses for orders 2 to 10.

2.2.2 Chebyshev type I filters (equal-ripple passband magnitude)

For the Butterworth response, $|K(j\omega)|^2$ is monotonically increasing. On contrary when a definite amount of ripple is allowed in the passband, some other functions can be utilized to construct a filter response. Instead of as in the equation (2.16)

$$|K(j\omega)|^2 = \varepsilon^2\omega^{2n} \tag{2.19}$$

The $|K(j\omega)|^2$ polynomial can be set as

$$|K(j\omega)|^2 = \varepsilon^2 C_n^2(\omega) \tag{2.20}$$

Where $C_n(\omega)$ is a confined function named Chebyshev polynomial expressed as

$$C_n^2(\omega) = \cos(n \cos^{-1} \omega) \quad \text{for } |\omega| \leq 1 \tag{2.21}$$

The Chebyshev magnitude response is

$$|T_n(j\omega)|^2 = \frac{1}{1 + \varepsilon^2 C_n^2(\omega)} \tag{2.22}$$

The ripples are confined between 1 and $1/\sqrt{1+\varepsilon^2}$ inside the passband and the response a steeper roll-off compared to the Butterworth response. In Figure 2.4, magnitude response for Chebyshev I filters, that has 1 dB passband ripple, with orders 2 to 10 can be seen.

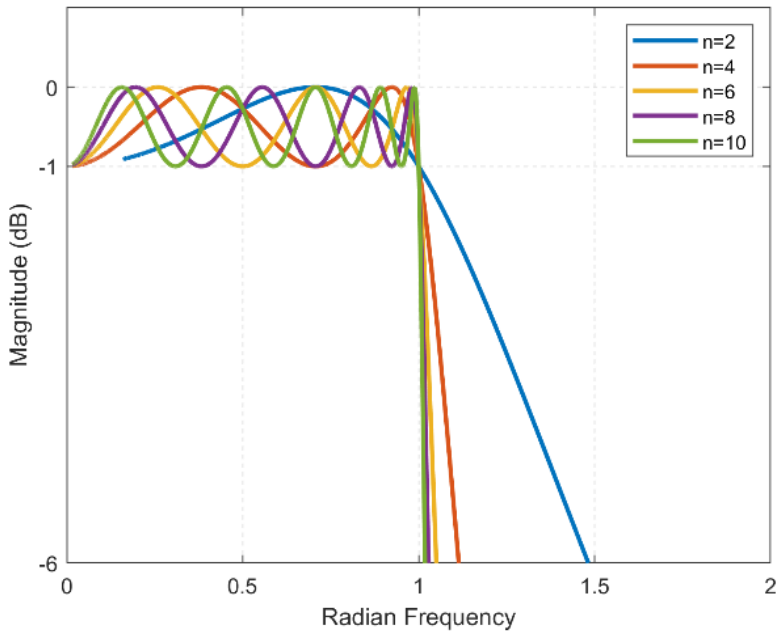

Figure 2.4 : Chebyshev type I magnitude responses for orders 2 to 10.

2.2.3 Chebyshev type II filters (equal-ripple stopband magnitude)

Starting from the equation (2.22)

$$|T_{C1}(j\omega)|^2 = \frac{1}{1 + \varepsilon^2 C_n^2(\omega)} \tag{2.23}$$

Which can be subtracted from 1 to obtain

$$1 - |T_{C1}(j\omega)|^2 = 1 - \frac{1}{1 + \varepsilon^2 C_n^2(\omega)} = \frac{1\varepsilon^2 C_n^2(\omega)}{1 + \varepsilon^2 C_n^2(\omega)} \tag{2.24}$$

Then replacing ω with $1/\omega$ to get a function as

$$|T_{C2}(j\omega)|^2 = \frac{1\varepsilon^2 C_n^2(1/\omega)}{1 + \varepsilon^2 C_n^2(1/\omega)} \tag{2.25}$$

which is called inverse Chebyshev (or Chebyshev II) response. This response has a flat behavior at the low frequencies and it has ripples at high frequencies opposite to Chebyshev I response. Ripples have a maximum at $\varepsilon^2/\sqrt{1+\varepsilon^2}$ at the stopband ($\omega \geq 1$).

In Figure 2.5, magnitude response for Chebyshev II filters having stopband ripple maximums at -30dB, with orders 2 to 10 can be seen.

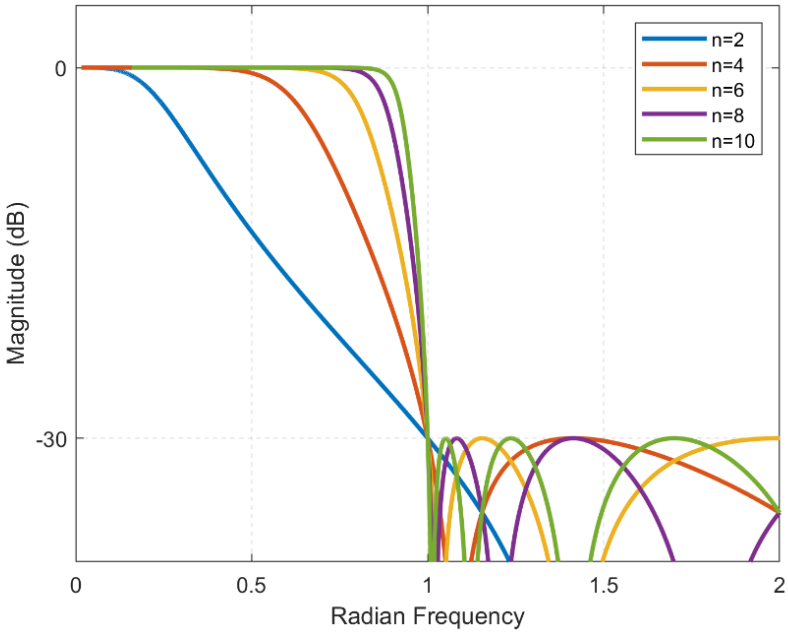

Figure 2.5 : Chebyshev type II magnitude responses for orders 2 to 10.

2.2.4 Cauer (elliptic) filters

In this type of response $|K(j\omega)|^2$ in the equation (2.10) is replaced by a function $|R_n(j\omega)|^2$. Where $R_n(j\omega)$ is equal to

$$|R_n(j\omega)| = \frac{A(j\omega)}{B(j\omega)} \tag{2.26}$$

Where poles and zeros are selected on the $j\omega$ axis to create equal ripples in passband and stopband both. In other words, Chebyshev type I and Chebyshev type II responses are fused together. In Figure 2.6 and Figure 2.7, magnitude response for Cauer filters that have stopband ripple maximums at -30dB and passband ripple of 1dB, with orders 2 to 10 can be seen.

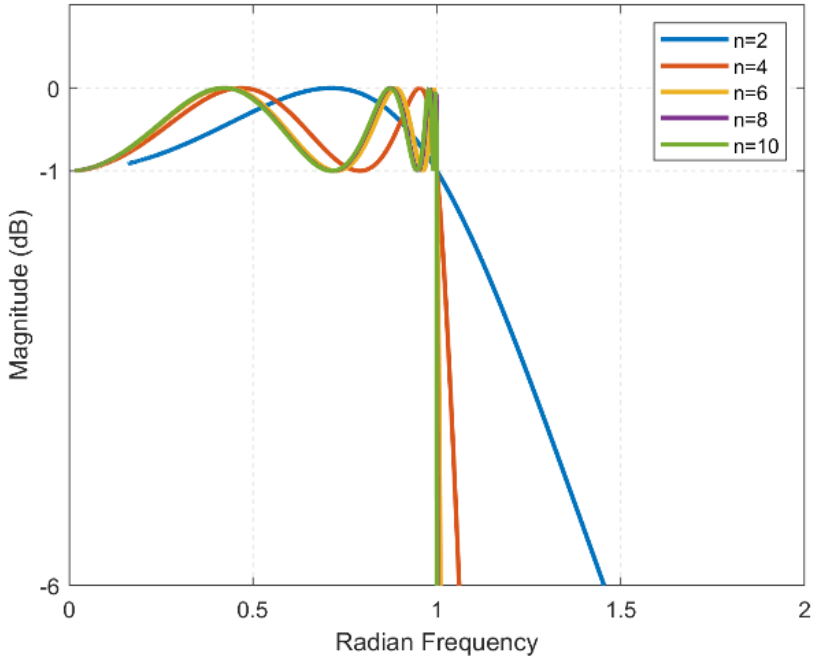

Figure 2.6 : Cauer magnitude response around passband for orders 2 to 10.

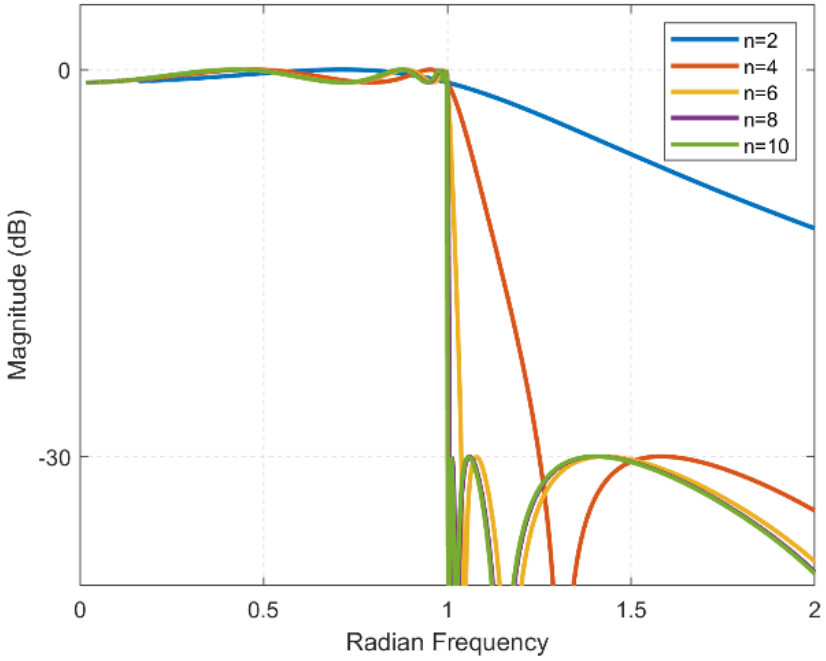

Figure 2.7 : Cauer magnitude response around stopband for orders 2 to 10.

2.3 Analog Filter Implementations

Filter functions are mathematical expressions. In order to be implemented in practical applications, these filter functions should be realized using real circuit elements. There are various ways of implementing a filter function. Passive circuit elements as resistors, capacitors, inductors can be used along with active circuit elements such as OTAs and switches. Depending on the circuit elements used, filters are categorized.

2.3.1 LC Ladder Filters

LC ladder filters are a type of passive filters which use no active elements that uses power. Independent of the order, LC ladder filters contain only two resistors. Other than the two resistors, there is also an LC ladder whose number of steps depends on the order of the filter. Values of the L and C elements are determined by the filter function which is to be implemented. In Figure 2.8, a block diagram for an LC ladder filter is illustrated.

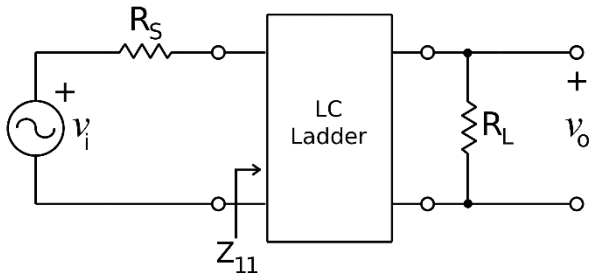

Figure 2.8 : LC ladder filter block diagram.

The reflection coefficient $A(j\omega)$ can be expressed as

$$A(j\omega) = \mp \frac{R_S - Z_{11}(j\omega)}{R_S + Z_{11}(j\omega)} \tag{2.27}$$

Meaning that

$$Z_{11}(j\omega) = R_S \left[\frac{1 - A(j\omega)}{1 + A(j\omega)}\right]^{\pm 1} \tag{2.28}$$

As an example, For a Butterworth filter for which

$$\left|\frac{V_o(j\omega)}{V_i(j\omega)}\right|^2 = \frac{K^2}{1+\omega^{2n}} \tag{2.29}$$

$|A(j\omega)|^2$ will be equal to

$$|A(j\omega)|^2 = \frac{\omega^{2n}}{1+\omega^{2n}} \tag{2.30}$$

When $R_L = R_S$, and $K = 1/2$ following equation will be correct

$$|A(j\omega)|^2 = \frac{\omega^n}{B_n(j\omega)} \tag{2.31}$$

where $B_n(j\omega)$ is the nth order Butterworth polynomial.

As an example, for a 3rd order Butterworth lowpass filter implementation will be as follows:

$$A(s) = \frac{s^3}{s^3+2s^2+2s+1} \tag{2.32}$$

From the equation (2.28)

$$Z_{11}(s) = \left[\frac{2s^2+2s+1}{2s^3+2s^2+2s+1}\right]^{\pm 1} = \frac{1}{s+\dfrac{1}{2s+\dfrac{1}{s+1}}} \tag{2.33}$$

Using the equations, this filter can be implemented as given in the Figure 2.9.

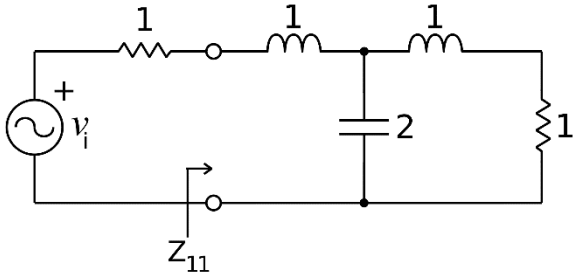

Figure 2.9 : Implemented LC filter.

Required L and C values for common filter responses are generated aforetime so that designers can utilize such tables for practical filter design. The two generalized

configurations for normalized LC ladder filter circuit diagrams are shown in Figure 2.10.

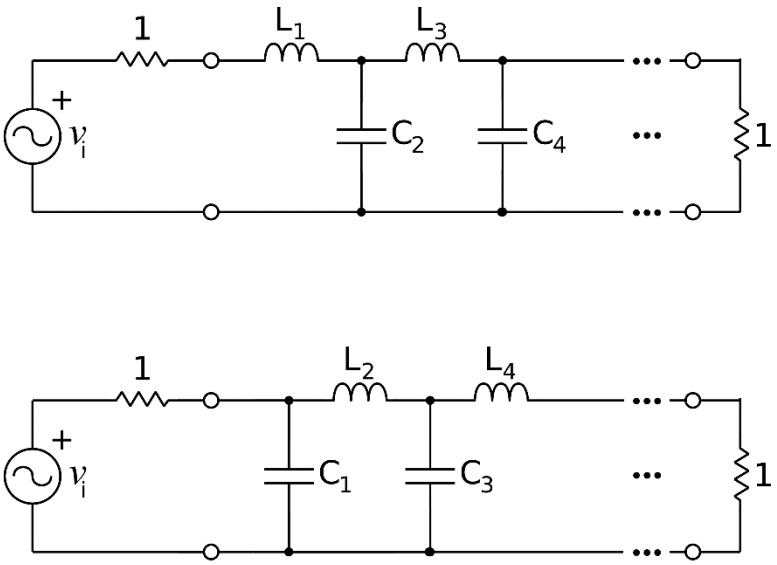

Figure 2.10 : Generalized LC ladder filter configurations.

2.3.2 Opamp-RC Filters

One way to realize filter functions is by using operational amplifiers. There are numerous ways to realize a second order filter function. Second order rational functions are referred as biquadratic functions, and circuits realizing these functions are called biquads. General form of a biquadratic function for a lowpass filter is stated as

$$T_{LP}(s) = \frac{A}{s^2 + \frac{\omega_0}{Q}s + {\omega_0}^2} \tag{2.34}$$

where Q is the quality factor of the biquad. Normalized second order lowpass functions with different Q values are shown in Figure 2.11 bellow.

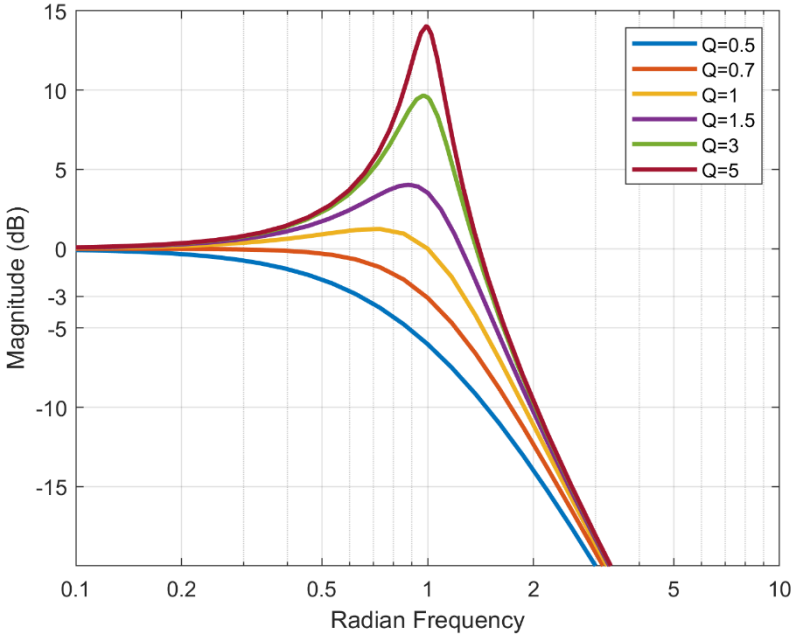

Figure 2.11 : Magnitude response of second order functions for different Q values.

It is critical that some circuits can implement such second order filter functions using operational amplifiers, since higher order filter functions can be broken down into a multiplication of multiple second order functions and one first order function if the function order is odd. This translates that by cascading the multiple second order filters (and a first order filter if the function order is odd), higher order filters can be implemented. This method provide useful since biquadratic filters are fairly straightforward to realize. There are various circuit topologies for implementation of biquadratic functions using operational amplifiers.

2.3.2.1 Tow-Thomas biquad

Tow-Thomas biquad circuit can be used for implementing a biquadratic filter function that has no finite transmission zeros. This means filter types such as Butterworth, Chebyshev Type I can be realized using a Tow-Thomas biquad. The circuit is shown in Figure 2.12. The transfer function of the lowpass output is as follows [10]

$$T_{LP}(s) = -\frac{\frac{R_6/R_4}{R_3R_1C_1C_2}}{s^2 + s\frac{1}{R_2C_1} + \frac{R_6/R_4}{R_3R_5C_1C_2}} \tag{2.35}$$

This means that

$$\omega_0 = \sqrt{\frac{R_6/R_4}{R_3 R_5 C_1 C_2}} \; and \; Q = \frac{R_2}{\sqrt{R_3 R_5}} \sqrt{\frac{R_6 C_1}{R_4 C_2}} \tag{2.36}$$

As can be seen in equations (2.35) and (2.36), Q and ω_0 values can be tuned independently. By adjusting the R_2 resistor, Q can be changed without effecting the pole frequency which clearly is an advantage for the designer.

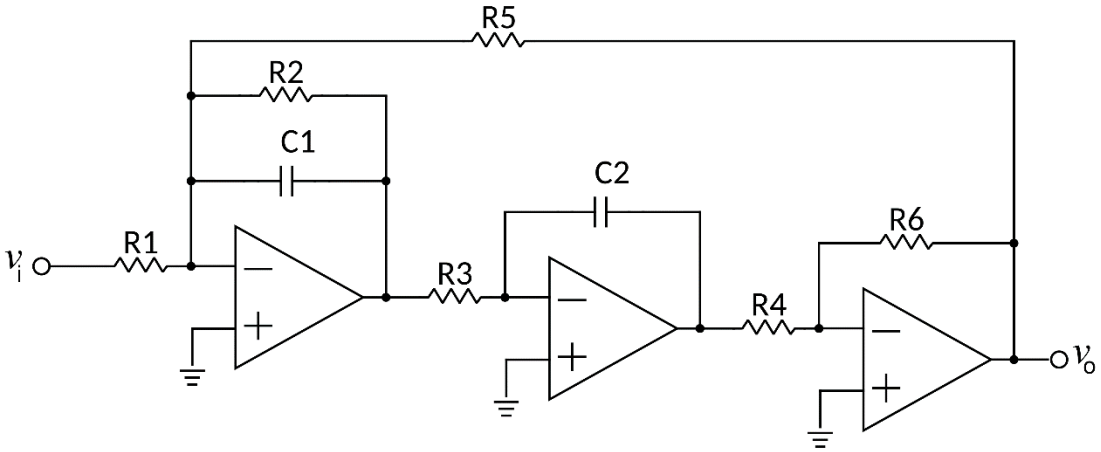

Figure 2.12 : Tow-Thomas filter circuit diagram.

Performance parameters such as dynamic range, supply noise rejection and harmonic distortion are greatly improved when fully differential topologies are utilized [11], [12]. In fully differential implementations of Tow-Thomas biquad, inverting operation done by the third operational amplifier will be accomplished by inverse connections therefore there will be only two operational amplifiers needed in the circuit.

2.3.2.2 Sallen-Key circuit

Some circuits can implement a second order filter function with only one operational amplifier. Sallen-Key topology is one of them. Circuit schematic is shown in Figure 2.13. Transfer function of the circuit is as follows [13]

$$T(s) = \frac{\frac{K}{R_1 R_2 C_1 C_2}}{s^2 + s\left(\frac{1-K}{R_2 C_2} + \frac{1}{R_1 C_1} + \frac{1}{R_2 C_1}\right) + \frac{1}{R_1 R_2 C_1 C_2}} \tag{2.37}$$

and

$$\omega_0 = \sqrt{\frac{1}{R_1 R_2 C_1 C_2}} \; and \; Q = \frac{\sqrt{\frac{1}{R_1 R_2 C_1 C_2}}}{\frac{1-K}{R_2 C_2} + \frac{1}{R_1 C_1} + \frac{1}{R_2 C_1}} \tag{2.38}$$

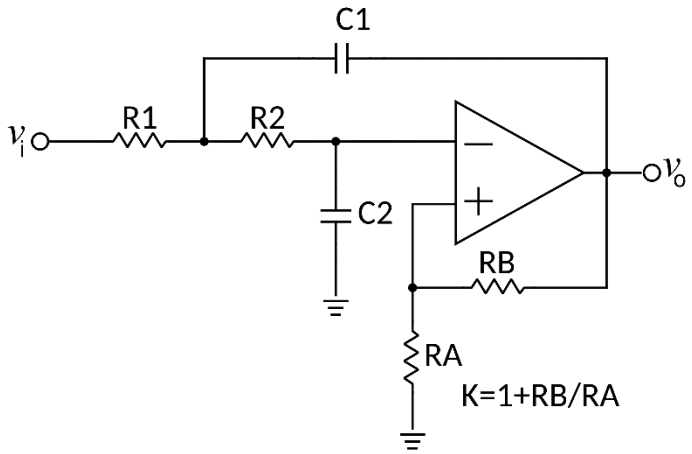

Figure 2.13 : Sallen-Key filter circuit diagram.

For the real differential implementation of Sallen-Key filters, differential difference amplifiers [14] which have four input nodes and two output nodes are required.

2.3.2.3 Multiple feedback circuit

Another type of biquad is the multiple feedback circuit. Multiple feedback circuit is a single operational amplifier filter. As the name suggests, there are more than one feedback across the operational amplifier. Circuit schematic for a lowpass multiple feedback filter is shown in Figure 2.14. Transfer function of the multiple feedback circuit is as follows [15]

$$T_{LP}(s) = \frac{\frac{1}{R_1 R_3 C_1 C_2}}{s^2 + s\left(\frac{1}{R_1 C_1} + \frac{1}{R_2 C_1} + \frac{1}{R_3 C_1}\right) + \frac{1}{R_2 R_3 C_1 C_2}} \tag{2.39}$$

and

$$\omega_0 = \sqrt{\frac{1}{R_2 R_3 C_1 C_2}} \; and \; Q = \sqrt{\frac{C_1/C_2}{\sqrt{R_3/R_2} + \sqrt{R_2/R_3} + \sqrt{R_2 R_3/R_1}}} \tag{2.40}$$

For the adjustment of Q without effecting the ω_0, R_1 value can be set independently.

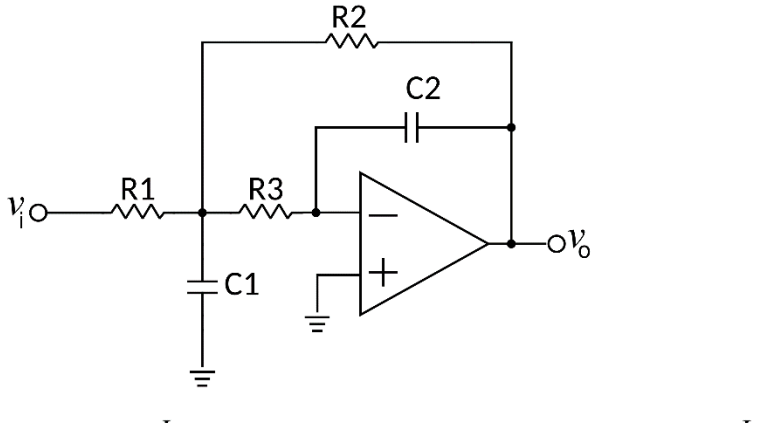

Figure 2.14 : Multiple feedback filter circuit diagram.

2.3.3 OTA-C filters

Basic filter elements such as resistors, inductors, integrators can be replaced with circuit elements that are created using transconductance amplifiers. By replacing these elements with their OTA-C equivalents, passive filters can be transformed into OTA-C filters. Since LC ladder filter can realize filter functions as described in earlier chapters, OTA-C filters can be implemented simply by replacing LC ladder elements with corresponding OTA-C equivalents. Equivalent circuits for a grounded resistor and a grounded inductor are interpreted in Figure 2.15 and 2.16 respectively.

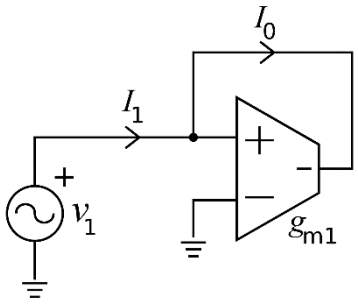

Figure 2.15 : OTA-C grounded resistor equivalent.

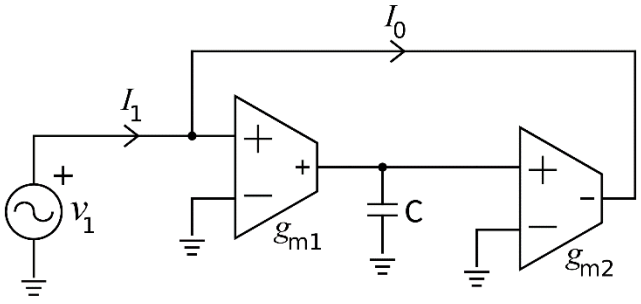

Figure 2.16 : OTA-C grounded inductor equivalent.

For the resistor equivalent circuit,

$$I_0 = g_m V_1 = I_1 \tag{2.41}$$

so

$$\frac{V_1}{I_1} = \frac{1}{g_m} = R_{eq} \tag{2.42}$$

For the inductor equivalent circuit,

$$V_x = g_{m1} V_1 \frac{1}{sC} \tag{2.43}$$

and

$$I_0 = g_{m2} V_x = I_1 \tag{2.44}$$

$$I_1 = g_{m2} g_{m1} V_1 \frac{1}{sC} \tag{2.45}$$

$$\frac{V_1}{I_1} = s \frac{C}{g_{m1} g_{m2}} = s\, L_{eq} \tag{2.46}$$

For OTA-C filters, circuit elements can be tuned via the g_m values and no inductors or resistors are required to be implemented in the filter.

2.3.4 Switched capacitor filters

Realizing resistors with switched capacitors, these filters can have very small corner frequencies without the need of large resistors. Additionally, frequency parameters will be very precise since clock frequencies which are generally created by crystal oscillators are very accurate and RC parameters depend on the ratios of the ratios of the capacitor values which is also very accurate. A switch capacitor equivalent of a resistor is shown in Figure 2.17. Φ_1 and Φ_2 are non-overlapping clock signals.

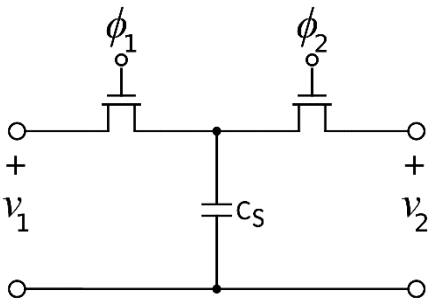

Figure 2.17 : Switched capacitor resistor equivalent.

From charge transfer,

$$\Delta q = q_1 - q_2 = (v_1 - v_2)C_S \tag{2.47}$$

When the frequency of the clock is much higher than the frequency of v_1 and v_2 sources (or signals), the equation can be approximated as

$$i \approx \frac{\Delta q}{T} = \Delta q \, f_C = f_C(v_1 - v_2)C_S \tag{2.48}$$

where T is the period and f_C is the frequency of the clock signal that flips the switches. Therefore, the equivalent resistance is

$$R_{eq} \approx \frac{v_1 - v_2}{i} = \frac{1}{f_C C_S} \tag{2.49}$$

This means that an RC time constant will be as

$$\tau_1 \approx \frac{C_1}{f_C C_S} \tag{2.50}$$

As an implementation example, a first order active filter circuit and its switched capacitor version are shown in the Figures 2.18 and 2.19 respectively.

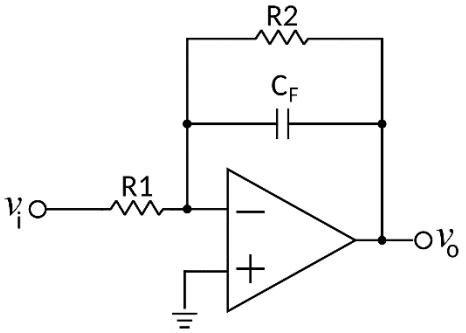

Figure 2.18 : First order active filter circuit diagram.

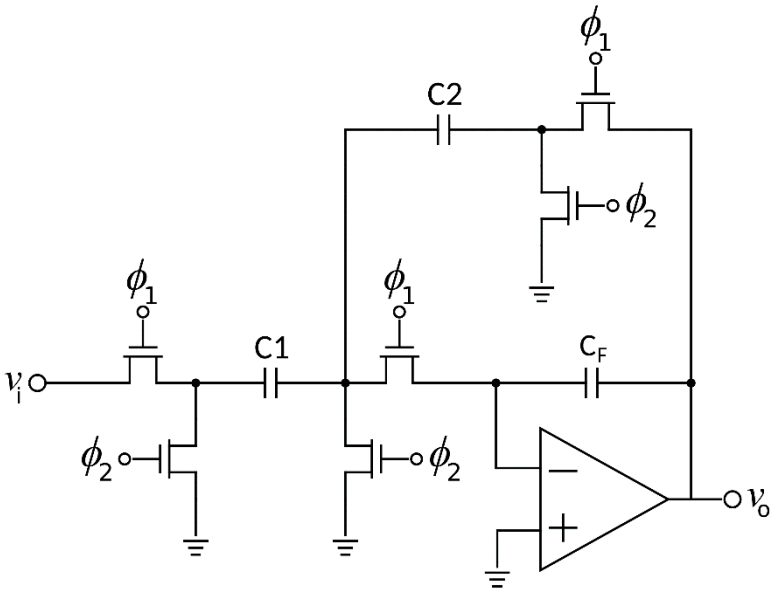

Figure 2.19 : Switched capacitor equivalent of first order active filter.

For the circuit in Figure 2.19, the transfer function will be as

$$T(s) = -\frac{1}{\frac{C_2}{C_1} + s\frac{C_f}{f_C C_1}} \tag{2.51}$$

so that a very accurate transfer function can be obtained which will depend on the ratios of the capacitor values.

2.4 Design Parameters of Analog Lowpass Filters

Analog filters have numerous requirements and restraints depending on the application and depending on the parts of the system which the filter will co-operate with. These requirements and restraints are defined for the system to be able to function properly as a whole. Such design parameters and performance metrics for analog lowpass filters will be defined in this chapter. Also, some of these parameters are illustrated in the Figure 2.20.

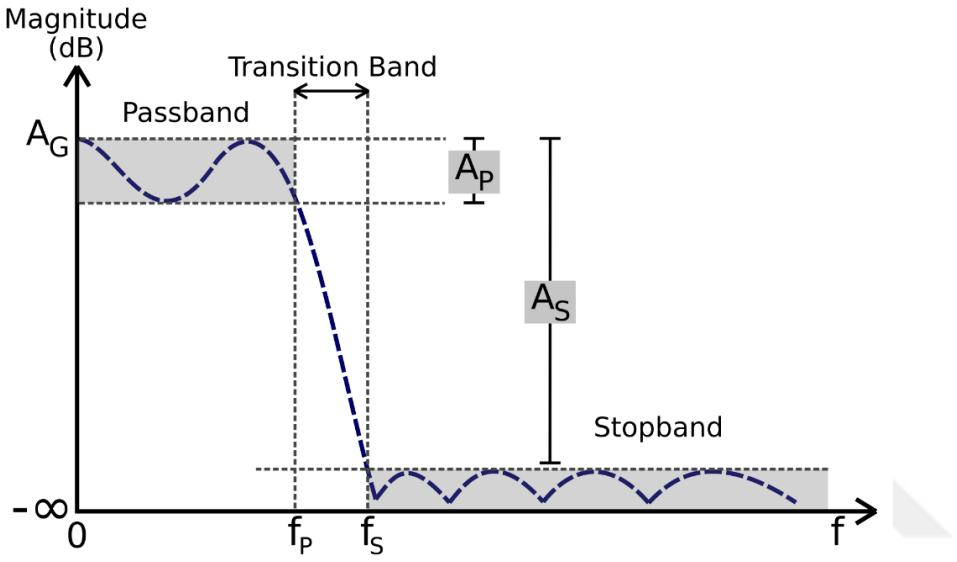

Figure 2.20 : Lowpass filter specification parameters.

2.4.1 Passband edge frequency

An analog lowpass filter is expected not to attenuate the input signals in a certain frequency band which is called the passband. The passband starts from the zero frequency and extends up to the passband edge frequency. Depicted as f_P in Figure 2.20.

2.4.2 Stopband edge frequency

For a lowpass filter the frequency band in which the signals are attenuated up to a desired point is called the stopband. Stopband ranges from the stopband edge frequency to the infinity. The frequency band between stopband edge and passband edge is called the transition band. Depicted as f_S in Figure 2.20.

2.4.3 Passband ripple

Magnitude fluctuations in the filter frequency response are called ripples. They are measured in dB. Ripples inside the passband are tagged as passband ripples. Certain amount of passband ripples can be tolerated in the filter. Depicted as A_P in Figure 2.20.

2.4.4 Stopband attenuation

Stopband attenuation is the measure of how much the signal is attenuated in the stopband, compared to the signal at the passband. Together with the width of the transition band, defines the required roll-off slope of the filter. Depicted as A_S in Figure 2.20.

2.4.5 Peak stopband ripple

There can be ripples in the stopband as well although this time the important parameter is not the amplitude od the ripple but its maximum value. This parameter should not exceed a certain value so that the stopband requirements will not be troubled.

2.4.6 Passband gain

Active filters can provide gain at the output compared to the input signal. The gain is the ratio of the amplitude of the signal at the output to the signal at the input. This gain is defined as a voltage gain and expressed in decibels. Depicted as A_G in Figure 2.20. The gain equation is shown as follows.

$$A_G = 20\log(|V_{OUT}/V_{IN}|) \tag{2.52}$$

2.4.7 Spurious free dynamic range (SFDR)

As a measure of linearity, the ratio of the fundamental output signal amplitude to the largest spur amplitude is called spurious free dynamic range. It is expressed in decibels. The equation is shown as below.

$$SFDR = 20\log\left(\left|V_{(Fundamental)}/V_{(Largest\ Spur)}\right|\right) \tag{2.53}$$

2.4.8 Effective number of bits (ENOB)

Ratio of the signal power to the power of the noise and distortion is called signal to noise and distortion ratio (SINAD). ENOB is calculated using the SINAD value and

helps to determine how much effective resolution bits can be obtained from the signal that is at the output of the filter. SNDR and ENOB are calculated as below.

$$SINAD = 10\log\left(\frac{P_{Signal}}{P_{Noise} + P_{Noise}}\right) \tag{2.54}$$

$$ENOB = \frac{SINAD - 1.76dB}{6.02dB} \tag{2.55}$$

2.4.9 Total harmonic distortion (THD)

Total harmonic distortion is the ratio of the total power of the harmonic signals to the power of the fundamental signal. Expressed in decibels or in percentage.

$$THD = 10\log\left(\frac{\sum P_{Harmonics}}{P_{Fundamental}}\right) \tag{2.56}$$

2.5 Fully Depleted Silicon on Insulator (FDSOI) Technology

When process variation, short channel effects and leakage currents are considered, fully depleted silicon on insulator technology provides better performance compared to the bulk CMOS technology therefore it is considered as an alternative to the further reduced bulk CMOS silicon geometries [16], [17], [18]. A thin layer of buried oxide layer (BOX) under the channel electrically isolates the bulk of the transistor from the channel resulting in reduced amount of leakage current. The undoped fully depleted channel is less prone to process variations compared to transistors with channel dopants which means reduced random dopant fluctuations (RDF). Since device channels are isolated from the bulk silicon, isolation between different devices is also improved. The buried oxide layer isolates the source and drain of the transistors from the substrate, so the parasitic diodes effects are lessened between source/drain and substrate. A cross-section of conventional-well FDSOI NMOS and PMOS devices is shown in Figure 2.21.

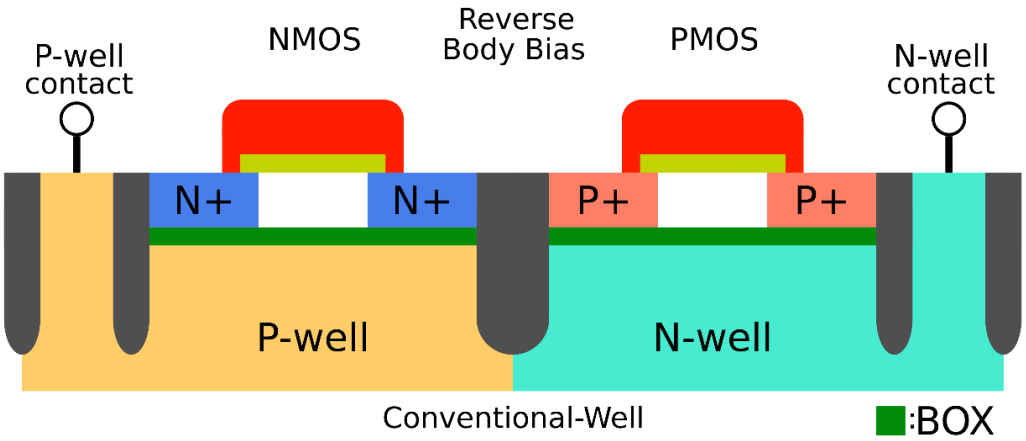

Figure 2.21 : Cross-section of conventional-well FDSOI process transistors.

One major advantage of an FDSOI MOSFET is that the body bias of the MOSFET device can be set freely since the channel of the MOSFET is isolated from the body. This also means that NMOS devices can be placed in NWELL instead of PWELL and similarly PMOS devices can be placed in a PWELL. This architecture is called flip-well and it allows threshold reduction by forward body biasing. Body biasing ability creates a design flexibility which can be utilized for bulk driving and threshold voltage shifting. A cross-section of flip-well FDSOI NMOS and PMOS devices is shown in Figure 2.22.

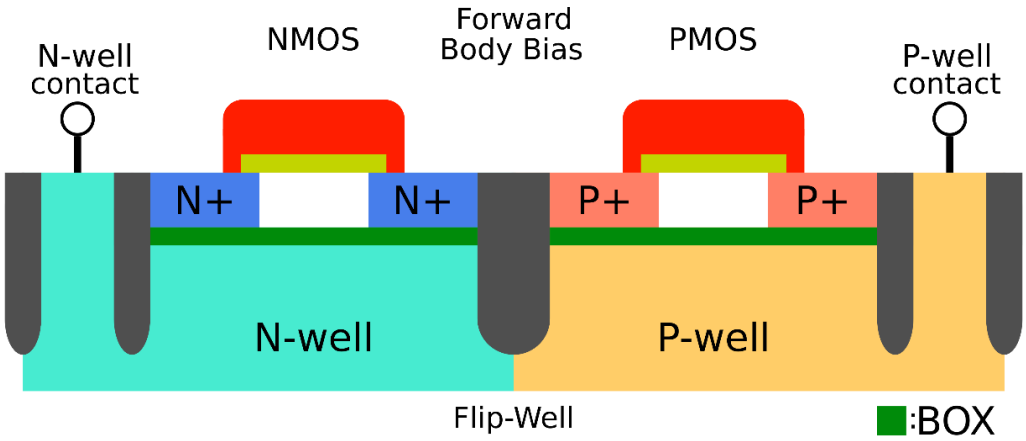

Figure 2.22 : Cross-section of flip-well FDSOI process transistors.

3. DESIGNED OPAMP-RC LOWPASS FILTER

The circuit is designed to be implemented on a mm-Wave 5G Multi-Input Multi-Output (MIMO) radio solution system-on-chip (SoC) as a baseband filter. It is required that the filter circuit needs to filter unwanted signals received from the RF receiver block and deliver the filtered signal to the ADC input. Consequently, the filter has requirements stated by the system design as well as the requirements stated by the RX and ADC blocks since there will be an interface on each side. In this chapter, design specifications and design the design of the opamp-RC filter in 22 nm FDSOI technology is explained.

3.1 Design Specifications

The opamp-RC lowpass filter is designed in 22nm FDSOI technology using the CADENCE design environment. The supply voltage domain is 0.8 V. The transistors used are the low voltage domain transistors with conventional-well and flip-well options.

The filter is required to have two operation modes one of which is the normal mode where the filter operates as a baseband filter with 12 dB gain and 25 MHz passband corner frequency. The passband corner frequency in this case defined as the frequency at which 1dB attenuation occurs. Stopband corner frequency is determined as 240 MHz and 60 dB attenuation compared to the passband is expected in the stopband. In this mode the passband ripple is expected to remain under 1dB. The output of the filter should have at least 7 effective resolution bits meaning that the ENOB of the filter output signal should more than 7 bits. Additionally, magnitude of the highest spur at the output of the filter should be 65 dB under the fundamental signal. This means that the SFDR at the output should be no less than 65 dB.

The second mode of operation is where the filter is used as a 0 dB gain buffer and the passband corner frequency shifted forward so that there will be no more than 1 dB attenuation up to 75 MHz (up to the third harmonic frequency of a 25 MHz signal). In this mode the passband is required to be flat. This mode is included in the design

because there is an application of the digital pre-distortion (DPD) technique in the receiver chain of the SoC.

These two modes of the filter will be referred as normal mode and DPD mode in this chapter. Since SFDR and ENOB parameters depend on the full-scale voltage level at the input of the filter, which is not specified at this stage of the project for the DPD mode, these parameters are not addressed in this thesis. Specifications for normal mode and DPD mode are given in Table 3.1 as below.

Table 3.1 : Design specifications of the filter.

Specification	Normal mode	DPD mode
1dB passband corner	> 25 MHz	> 75 MHz
Stopband corner	< 240 MHz	-
Stopband attenuation	> 60 dB	-
Passband ripple	< ∓ 1 dB	< ∓ 1 dB
SFDR	> 65 dB	-*
ENOB	> 7 bits	-*
Power consumption	< 10 mW	< 10 mW

*Unspecified at this stage of the project

Considering the specifications, a continuous time analog filter is designed. Continuous time analog filters are convenient choices for high frequency and high dynamic range filtering [19], [20]. The designed filter is a 4th order opamp-RC lowpass filter. Designed 4th order filter consists of two sub-blocks. These sub-blocks are a 3rd order Chebyshev type I lowpass filter followed by a variable gain first order lowpass filter both of which are implemented as opamp-RC configurations. The required passband corner frequency and stopband attenuation is provided by the 3rd order lowpass filter while the variable gain first order filter also contributes the attenuation. Variable gain first order filter provides 12 dB gain in normal mode and drives the ADC which is the load for the filter circuit. These circuits are designed together to have the desired specifications.

3.2 3rd Order Chebyshev Type I Filter

In order to provide the required stopband attenuation and passband corner frequency while confining the passband ripple, a 3rd order Chebyshev Type I Filter with a passband corner frequency of 25 MHz is designed. The passive RC circuit followed by a Tow-Thomas biquad together creates a 3rd order filter with a Chebyshev type I response. Schematic view of the 3rd order filter circuit is shown in Figure 3.1.

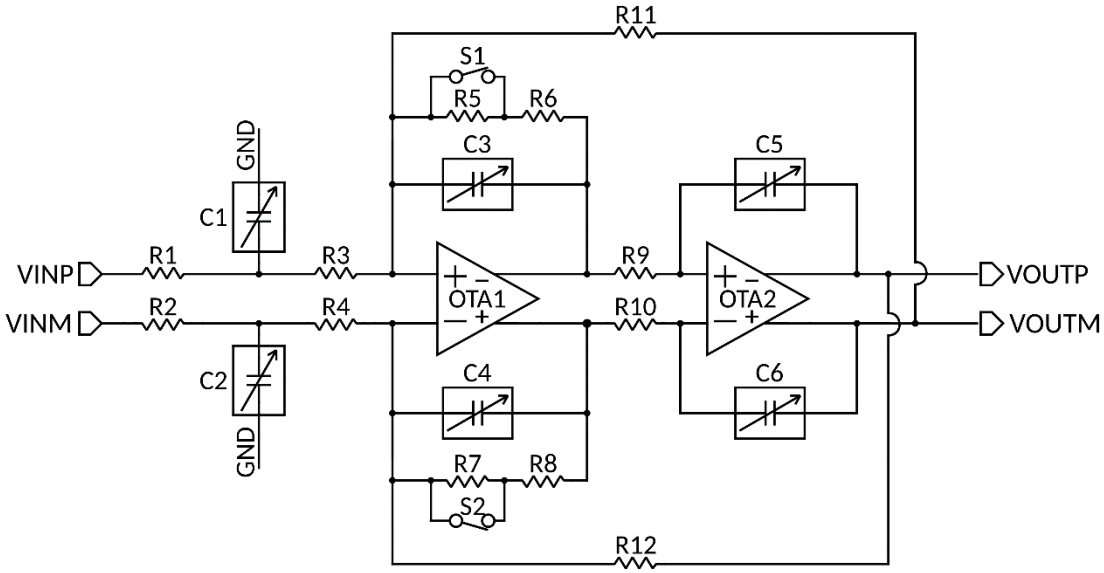

Figure 3.1 : 3rd order filter circuit diagram.

The frequency response of the filter is determined by the resistor and capacitor values which suffer from process variations. For this reason, a calibration method is implemented to compensate the effect of process variation on the filter response. In order to calibrate the filter frequency response, the capacitors are designed as switchable capacitors controlled by Serial Peripheral Interface (SPI) so that the RC product can be kept in a desired interval. Moreover, in the DPD mode where passband corner frequency is shifted above 75 MHz, switchable capacitors are adjusted to reduce the capacitance values of the filter. Schematic of the switchable capacitor blocks and schematic of the switches used in the switchable capacitor blocks can be seen in Figure 3.2.

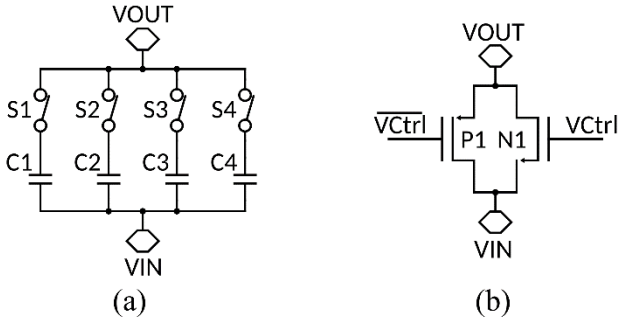

Figure 3.2 : Circuit diagrams of a) Switchable capacitor and b) CMOS switch.

In order obtain a flat passband in the DPD mode, Q defining resistor of the Tow-Thomas biquad is designed to be adjustable. The S1 and S2 switches in the Figure 3.1 are switched ON to decrease the Q defining resistor value by bypassing the R5 and R7

resistors. Thus, a more Butterworth-like flat passband filter characteristics is obtained in DPD mode.

3.2.1 Operational amplifier

Operational amplifier is a critical part of the biquad. For the non-ideal operational amplifiers' effect on the transfer function of the filter to be negligible, designed operational amplifier must have a gain-bandwidth product around 100 times the filter passband corner frequency [21], [22], [23]. In this case, the amplifier is designed to have 2.5 GHz gain-bandwidth product. Additionally, the open-loop DC gain of the amplifier is designed to be more than 60 dB to prevent the excessive passband ripples. In the aspect of time domain behavior, the amplifier should be able to operate without generating too much high order harmonics at the output so that the filter can satisfy the linearity requirements and the noise generated by the amplifier should not compromise the filter's ENOB specification. Also, since operational amplifiers' power consumption is restricted by the filter specifications.

The designed operational amplifier is a fully differential two stage transconductance amplifier. The first stage is a folded cascode input stage while the second stage is a class AB output stage. Also, a common-mode feedback circuit is included since the designed amplifier is fully differential. In an effort to reduce the threshold voltages, all transistors in this design are in flip-well configuration where NMOS are in NWELL biased with VDD and PMOS are in PWELL biased with GND. Total power consumed by one operational amplifier is 2.6 mW. Power breakdown table can be seen in Table 3.2.

Table 3.2 : OTA power breakdown table.

Total Power	Biasing	CMFB	Stage 1	Stage 2
2.6 mW	0.24 mW	0.2 mW	0.96 mW	1.2 mW

3.2.1.1 Folded cascode input stage

First stage of the operational amplifier is a rail-to-rail input folded cascode stage as shown in Figure 3.3. Rail to rail input with input transistors N1, N2 and P1, P2 assures that the filter can function properly with wide range of input common-mode levels. Folded cascode structure provides gain without contributing to the noise. N6, N10 and

P7, P12 transistors create floating current mirrors to bias the output stage. P4, P5, P10 and P9 transistors are biased by the common-mode feedback circuit so that the output common-mode voltage level is set to a desired value.

In terms of noise, the critical transistors in the design are N8 and N4 mosfets. The flicker noise of these transistors has the highest contribution to the integrated output noise of the operational amplifier. In order to further improve the noise performance of the operational amplifier, N8 and N4 transistors can be replaced with larger area transistors. This way the flicker noise will be reduced with a cost of power consumption.

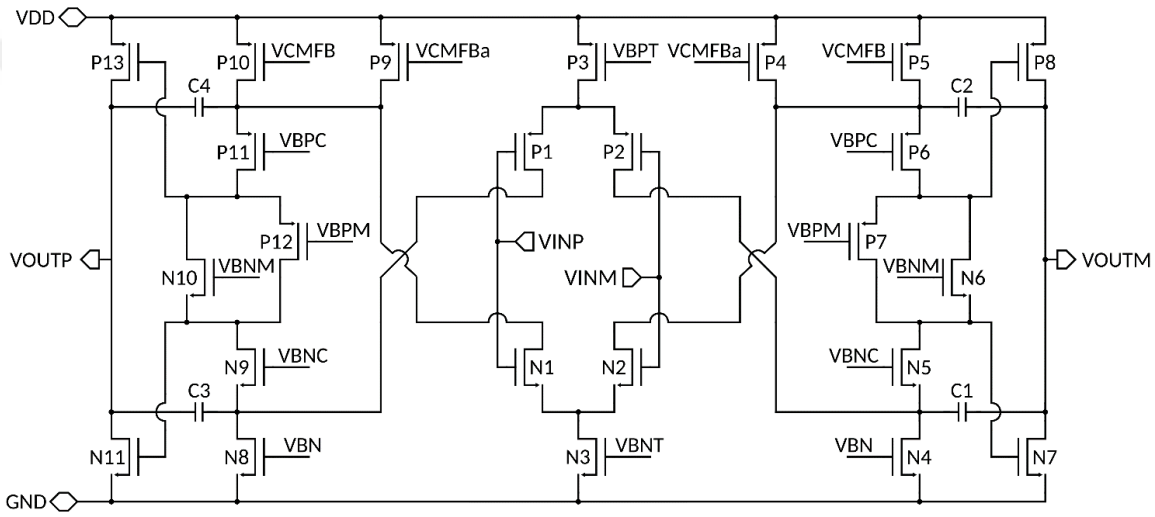

Figure 3.3 : Operational amplifier first and second stage circuit diagram.

3.2.1.2 Class AB output stage

N7, N11 and P8, P13 transistors in the Figure 3.3 are the output stage transistors of the operational amplifier. This is a class AB output stage first introduced by Monticelli [24]. The output stage contributes to the gain while allowing a rail-to-rail swing at the output and high slew-rate so that the linearity of the signals at the output is not compromised. Since the amplifier has two gain stages, compensation is required for bringing the dominant pole closer to zero (away from the second pole) to ensure the stability of the amplifier.

3.2.1.3 Common-mode feedback circuit

Operational amplifier being fully differential, a common-mode feedback circuitry is required to set the output common-mode voltage to a desired value. A modified 5-transistor OTA is used as an error amplifier as shown in Figure 3.4. Transistors P15 and P17 are employed to imitate the P6, P11 cascode transistors of the differential amplifier so that the common-mode error is reduced.

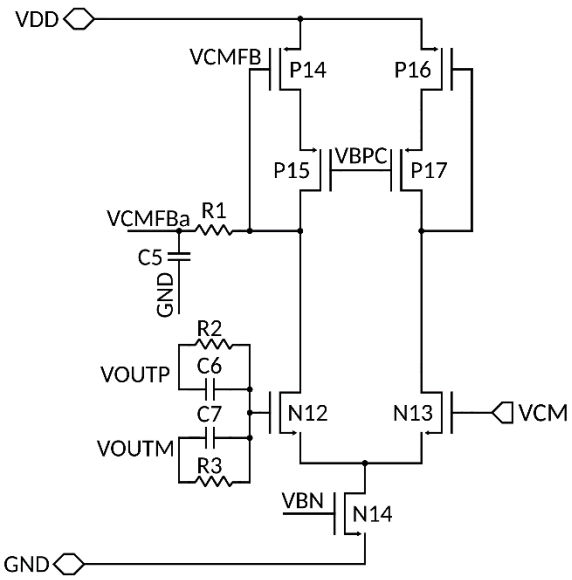

Figure 3.4 : Common-mode feedback circuit diagram.

The stability of the common-mode feedback loop is ensured by the same compensation capacitors that compensate the open loop amplifier response. This means that in order to improve the stability of the common-mode feedback loop, the compensation capacitance of the OTA must be increased. On the other hand, this will decrease the gain-bandwidth product of the differential amplifier which is not desirable. For this reason, a multi-path common-mode feedback is used for further improving the stability of the common-mode feedback circuit without effecting the differential mode open-loop response [25]. Output of the error amplifier is fed to the bias transistors in two branches. P4, P10 transistors in Figure 3.3 are biased by the error amplifier output node named CMFB and P9, P10 transistors are biased by the RC filtered error amplifier output node named CMFBa. This way without decreasing the low frequency gain of the common-mode feedback loop, the stability is increased with a cost of a slight reduction in common-mode gain-bandwidth product.

3.2.1.4 Bias generation

Gate bias voltages of tail and cascode transistors of the operational amplifier are generated by the bias generation part. As shown in Figure 3.5 two input current branches receive reference currents to generate bias voltages for the operational amplifier circuit. N25, N26 and P22, P23 transistors imitate the differential input transistors to generate biases for the tail transistors of the differential input stage. Diode connected N30 and P27 transistors generate the bias voltages for the floating current sources. While diode connected N15 and P18 transistors generate gate voltages for cascode transistors, N16 and P19 transistors generate gate voltages for cascode tail transistors.

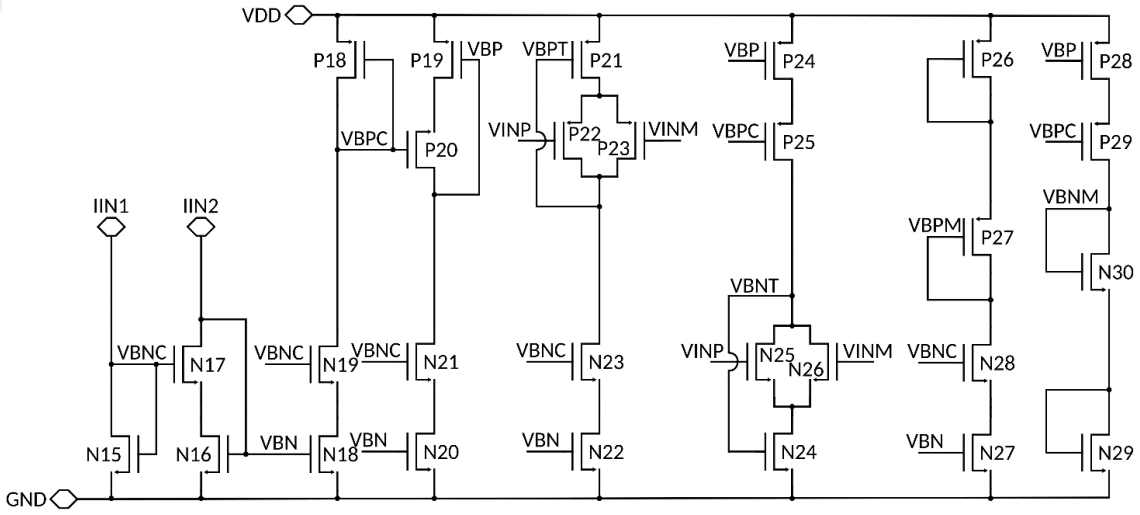

Figure 3.5 : Bias generation circuit diagram.

3.3 Variable Gain First Order Amplifier

The variable gain first order filter is a first order opamp-RC lowpass filter which has a passband corner frequency at 60 MHz. It contributes to the stopband attenuation of the 4th order filter without affecting the passband corner frequency, provides gain to the input signal, and calibrates the output offset caused by the preceding 3rd order filter block and by the gain amplifier itself. Schematic of the circuit is shown in Figure 3.6. Transistors R3 and R6 are switchable resistors which can take three different values to create 3 different gain options. 12 dB, 6dB and 0dB gain options can be selected by the changing the assigned SPI bits. In the normal mode of the 4th order filter, 12 dB

option is selected. 6 dB and 0dB gain options are implemented for testing and debugging purposes. 0 dB gain option is selected also in the DPD mode. Additionally, in the DPD mode, C1 and C4 capacitors are switched OFF to shift the passband corner frequency of the first order filter to a very high frequency (above 75 MHz).

The same operational amplifier used in the 3rd order filter block is used in the variable gain amplifier. Additionally, there are two offset calibration circuits in the variable gain first order filter.

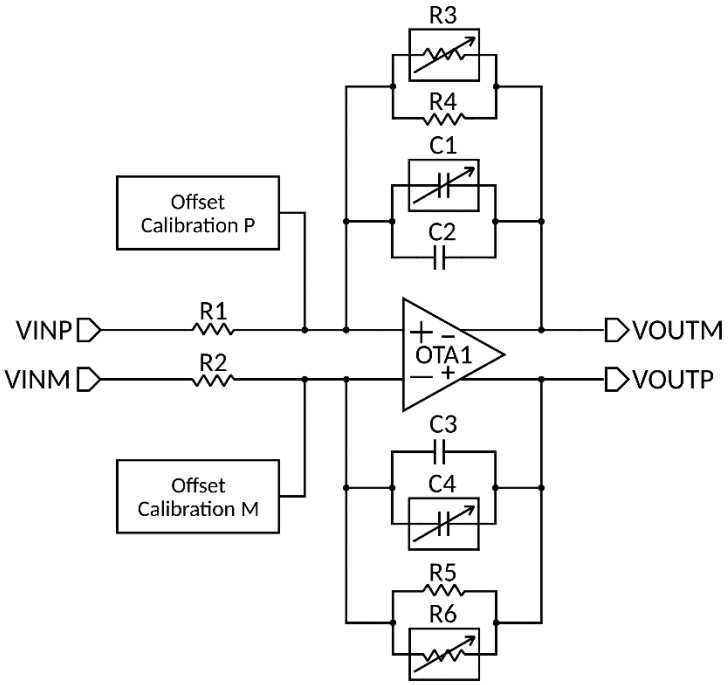

Figure 3.6 : First order variable gain filter circuit diagram.

3.3.1 Offset calibration circuit

The offset created by the 3rd order filter and the variable gain first order filter amplifier blocks because of the mismatch of the circuit elements is calibrated by the mismatch calibration circuits. Schematic of a mismatch calibration circuit is shown in Figure 3.7. In the offset calibration circuit either NMOS devices or PMOS devices are active meaning that the circuit has two operating modes. One mode is current sinking mode in which a controlled amount of DC current is sunk from the output node. The other mode is current sourcing mode where a controlled amount of DC current is sourced to the output node. The amount of current sunk or sourced is controlled by 7 dedicated

SPI bits controlling the gate voltages of binary weighed N1-6 and P1-6 transistors to obtain 128 levels of calibration (64 positive and 64 negative offset levels).

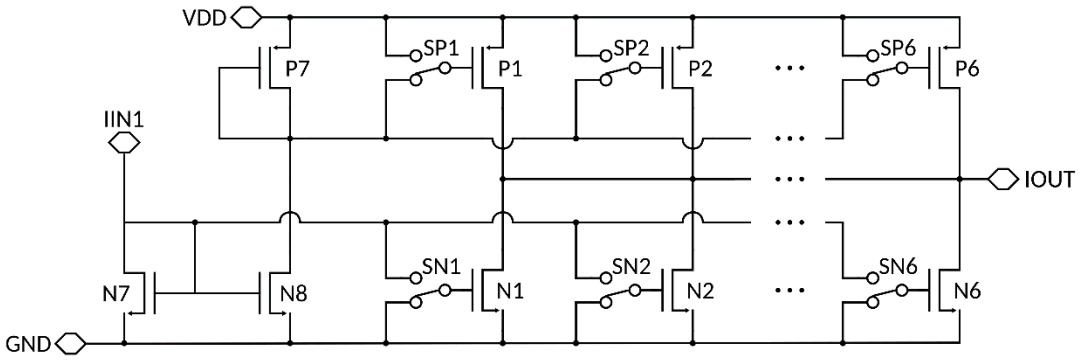

Figure 3.7 : Offset calibration circuit diagram.

There are two offset calibration circuits in the variable gain amplifier which are connected to the differential input nodes of the operational amplifier. While one of the offset calibration circuits is in current sinking mode, the other one is in current sourcing mode. Two offset calibration circuits sink and source equal amounts of DC currents. Since equal amounts of DC currents are sunk and sourced, there is no common-mode shift introduced at the inputs of the operational amplifier but a DC offset is created. DC offset shift provided to the inputs of the operational amplifier will be reflected at the output of the variable gain first order filter. By setting the offset calibration bits properly, DC offset at the output of the 4th order filter caused by mismatch can be reduced below 5 mV by the offset calibration circuits.

3.4 Simulations

Simulation results for the designed operational amplifier and the 4th order filter are presented in this chapter. Since the operational amplifier is a critical part of the design, its simulation results are shown apart from the simulations of the 4th order filter.

Open loop gain and phase of the designed operational amplifier are shown in Figure 3.8. Load capacitance for this simulation is chosen as 1pF because the operational amplifiers in the filter are required to be able to drive 1pF capacitors of the lowpass filter circuit without any stability issues. Obtained 70 dB DC gain, 2.55 GHz gain-bandwidth product and 62.7° phase margin values can be seen in the Figure 3.8 for the total power consumption of 2.26 mW.

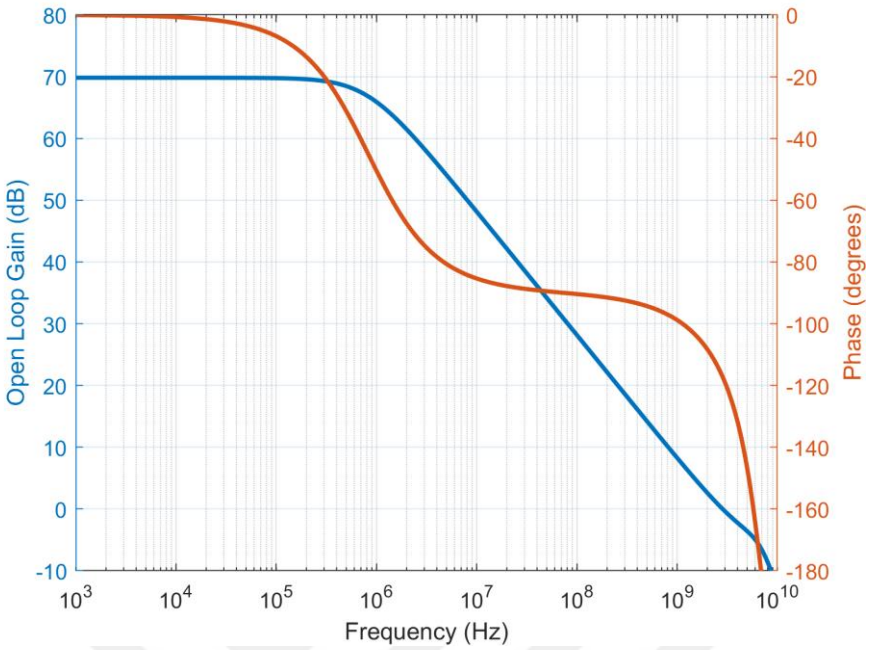

Figure 3.8 : Open loop response of the operational amplifier.

Step response of the operational amplifier for a 400 mV amplitude differential input voltage is shown in Figure 3.9 below.

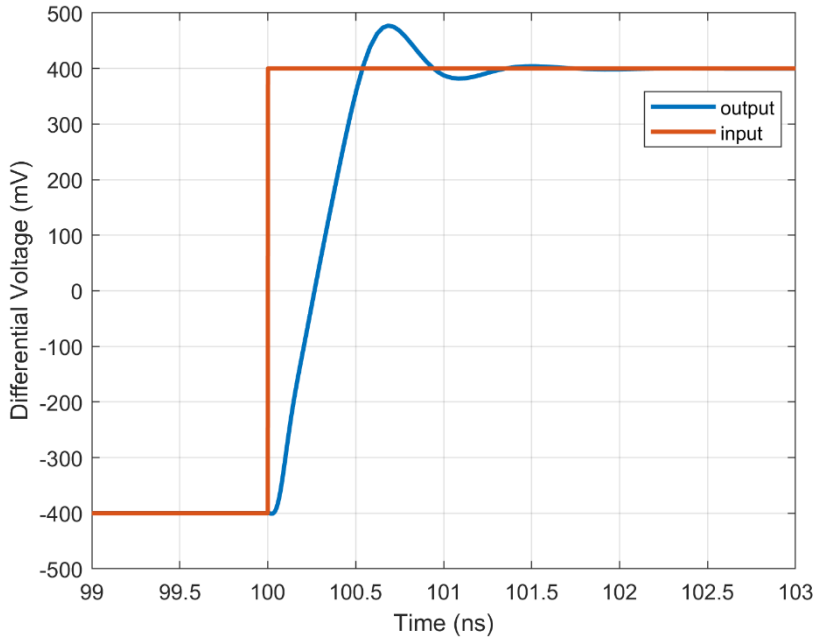

Figure 3.9 : Step response of the operational amplifier.

Frequency responses of the 4th order lowpass filter in normal mode for typical, RC max and RC min process corners are shown in Figure 3.10 and 3.11. Frequency

responses around passband corner and stopband corner are shown in Figure 3.10 and Figure 3.11 respectively. Additionally, frequency responses obtained after the calibration for RC max and RC min process corners are shown as well. Green sold line is the filter response in typical process corner. Dotted red and blue lines are frequency responses in RC min and RC max corners when there is no calibration and solid red and blue lines are frequency responses after the frequency calibration obtained by changing the SPI control bits of the switchable capacitor circuits accordingly.

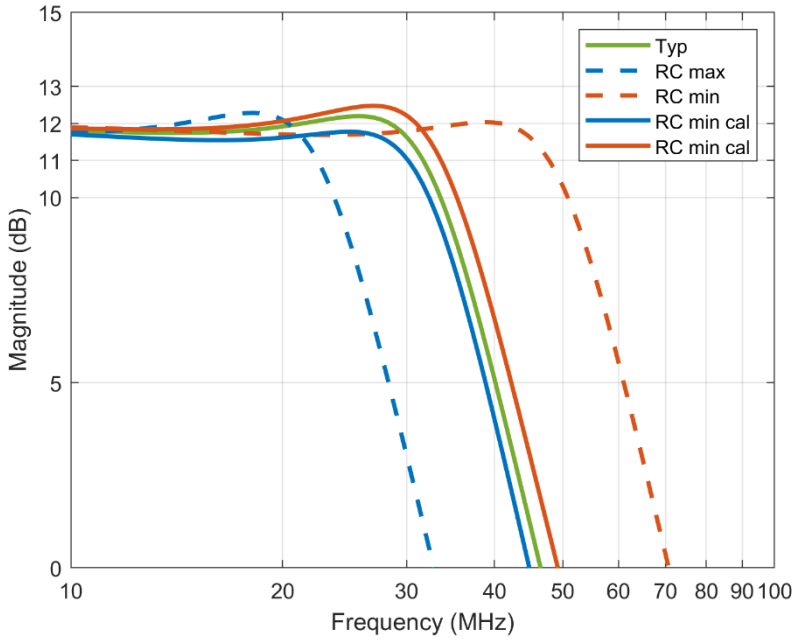

Figure 3.10 : Frequency response of the lowpass filter around passband corner.

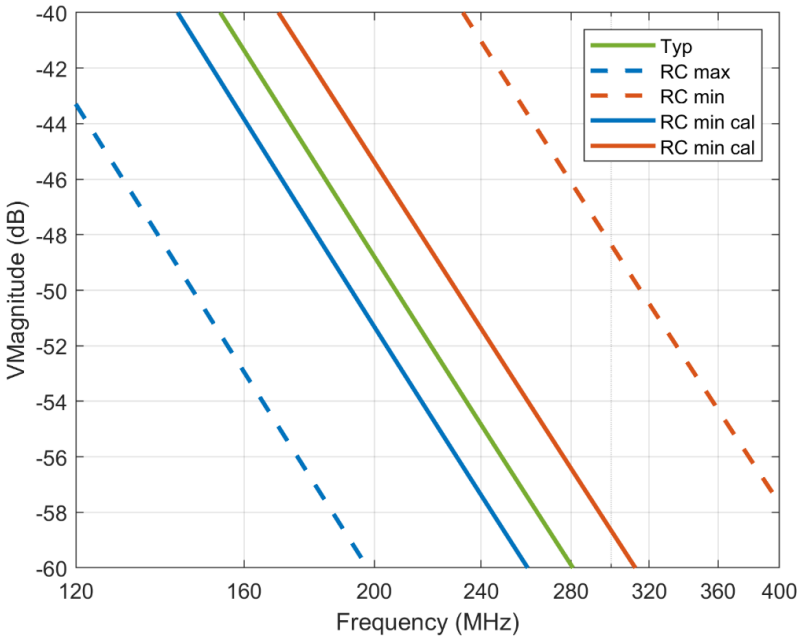

Figure 3.11 : Frequency response of the lowpass filter around stopband corner.

With the calibration capability of the filter, passband frequency higher than 25 MHz, stopband attenuation more than 60 dB and passband ripples less than 1dB are obtained for every process corner.

4th order filter transient input and output waveforms for three different gain options are shown in Figure 3.12 below. 12 dB option is for the normal mode of operation and other gain options are used for testing and debugging purposes. Input signal in this simulation is a sinusoidal signal with the frequency of 3.516 MHz and 100 mV differential amplitude which is the defined full-scale input voltage for the lowpass filter circuit.

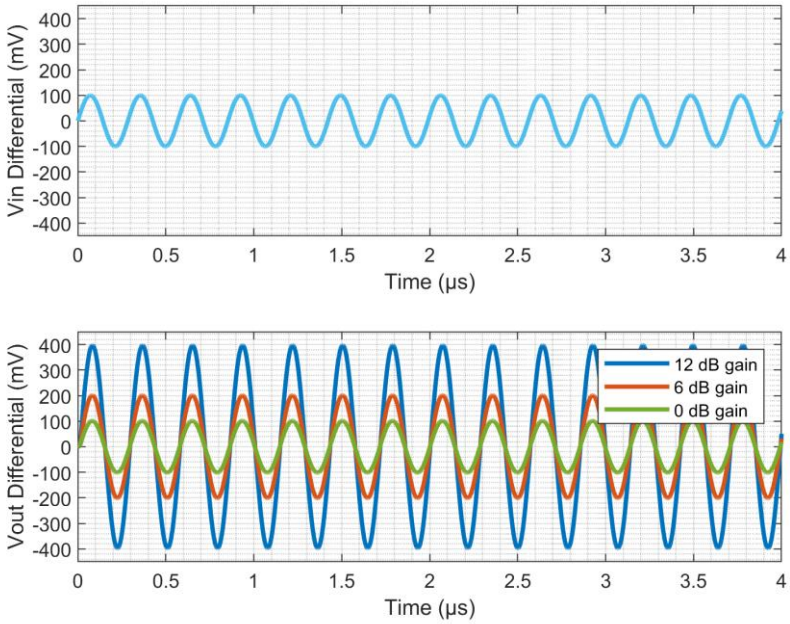

Figure 3.12 : Input and output signal waveforms for different gain options.

Frequency spectrum for the output signal of the filter, when a 100 mV differential sinusoidal signal with 25.08 MHz frequency is applied to the input, is shown in Figure 3.13. At the output of the filter, the magnitude of the fundamental signal is -7.8 dBc which corresponds to 407 mV differential signal (0 dBc corresponds to 1V). As can be seen in Figure 3.13, the highest spur is at 75.24 MHz with a magnitude of -89.2 dBc. This is expected since the 75.24 MHz is the closest odd harmonic frequency, which is the third harmonic, of the fundamental signal. Since the filter is fully differential, the second order harmonic magnitude remains under the third harmonic.

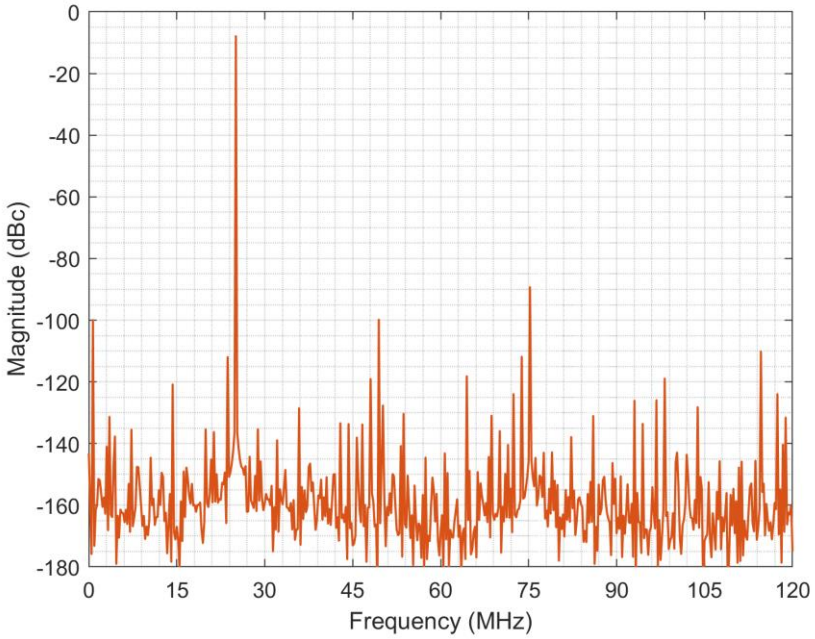

Figure 3.13 : Frequency spectrum of the output signal.

ENOB and SFDR values obtained from the transient simulations are shown in Figure 3.14 and Figure 3.15. Figures show ENOB and SFDR values for different input/output frequencies. Input signal amplitude for the simulations is the full-scale amplitude which corresponds to 100 mV differential and the signal amplitude produced at the output is around 400 mV differential since the filter gain is 12 dB.

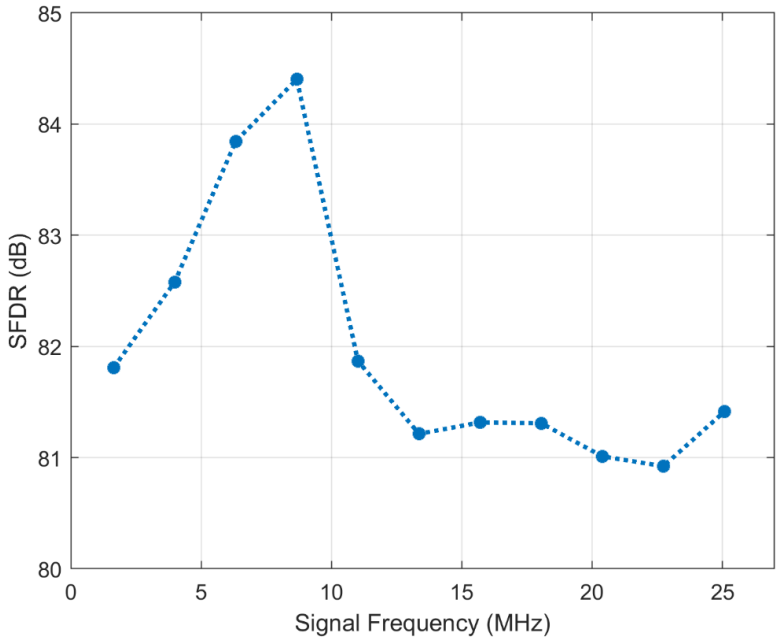

Figure 3.14 : SFDR values for different input signal frequencies.

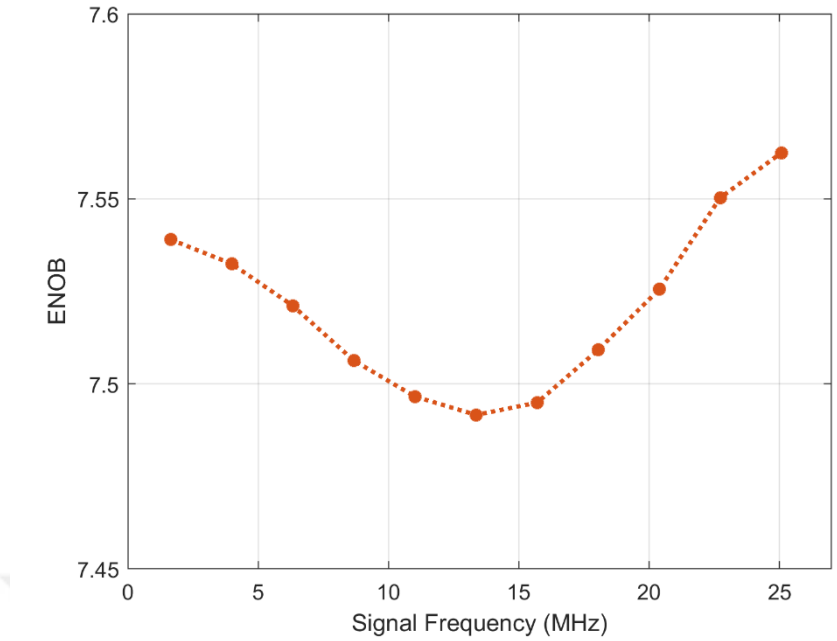

Figure 3.15 : ENOB values for different input signal frequencies.

Offset calibration capability of the filter is demonstrated in Figure 3.16. For different SPI bit values, obtained DC offset shift is shown. 128 different levels of offset shift can be achieved with 5 mV steps.

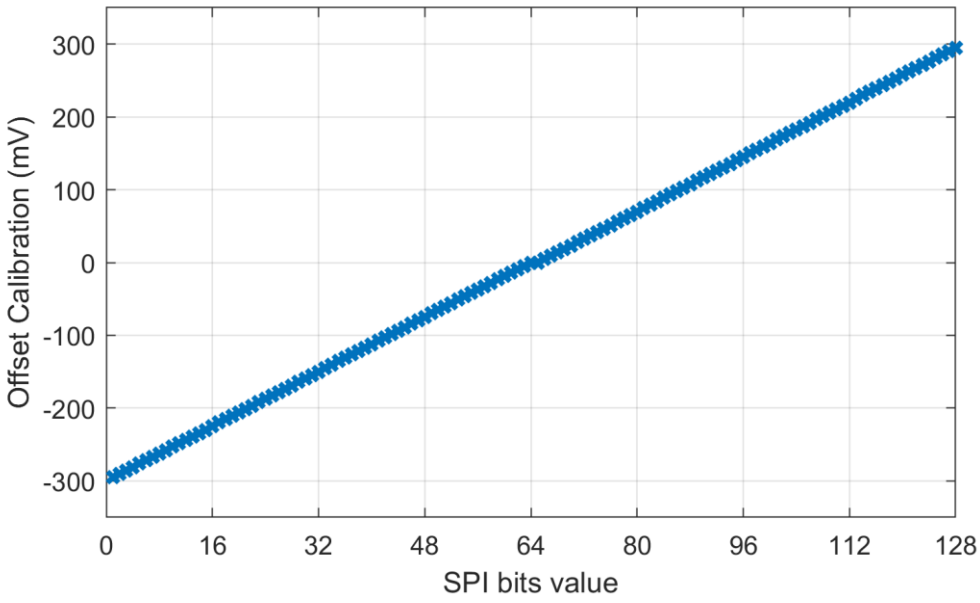

Figure 3.16 : Offset shift for different SPI bit values.

For the DPD mode of the circuit, frequency response is shown in Figure 3.17 below. Filter gain is reduced to 0dB and the passband corner frequency is shifted above 75 MHz. Since the Q defining resistor is reduced in the DPD mode, a flat passband response is obtained.

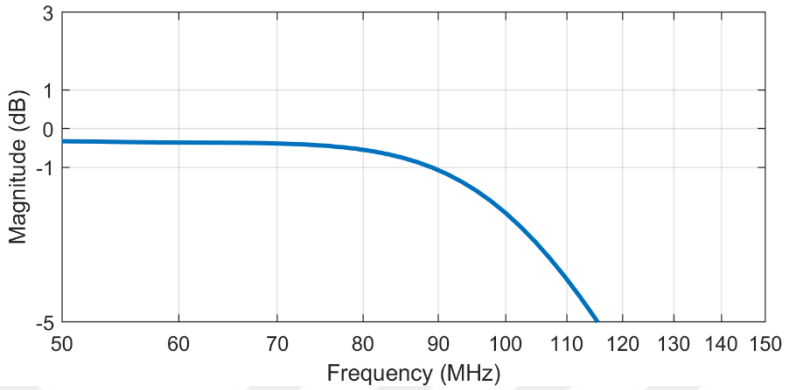

Figure 3.17 : Filter frequency response in DPD mode.

DPD mode transient input and output waveforms are shown in Figure 3.18. The input signal for the simulation is a 100 mV differential amplitude sinusoidal signal with 70.54 MHz frequency.

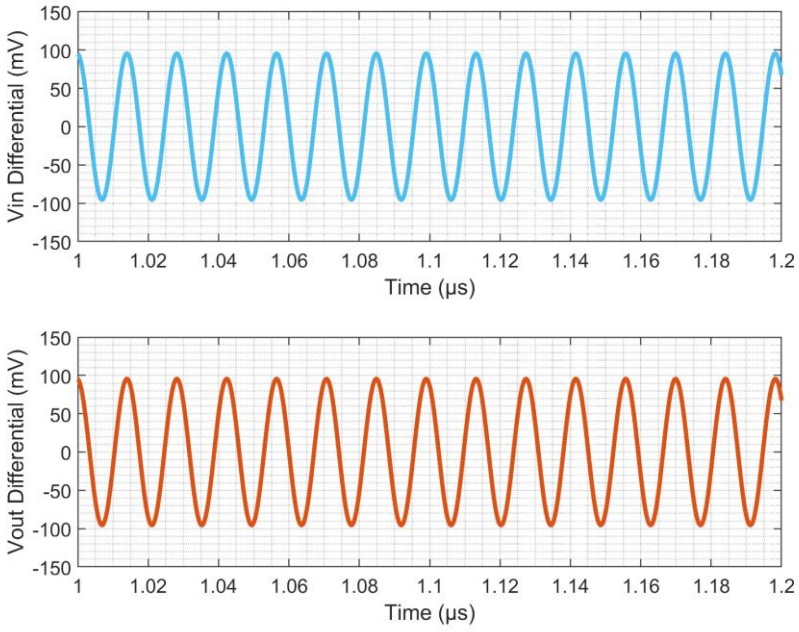

Figure 3.18 : Input and output signal waveforms in DPD mode.

In the Table 3.3, comparison of performance parameters for the designed filter and referred filters in the literature is shown.

Table 3.3 : Filter performance comparison.

Parameters	This Work	[26]	[27]	[28]	[29]	[6]	[30]
Technology	22 nm	130 nm	130 nm	130 nm	65 nm	120 nm	90 nm
F_{cutoff} - 3dB (MHz)	31	20	40	11.3	70	5	7
Topology	Active-RC	Active-RC	Active-RC	Active-RC	PWM	Active-RC	Ring Oscillator
VDD (V)	0.8	1.0	0.6	0.55	0.6	1.0	0.55
Order	4th	5th	4th	4th	4th	5th	4th
Response	Ch.	Ch.	But.	But.	But.	Che.	But.
SFDR (dB)	81.4	-	60.7	-	65.0	73.0	67.5
SNR (dB)	47.2	-	57.2	-	55.8	-	61.4
SNDR (dB)	47.1	40.0	55,6	40.0	54.4	40.0	58.0
ENOB	7.53	6.35	8.94	6.35	8.70	6.35	9.30
Power (mW)	7.8	7.5	10,6	3.5	26.2	6.1	2.9
VFS (% of VDD)	50	-	48	25	73	35	28
Area (mm^2)	0.06	1.94	0.24	0.43	0.38	0.25	0.29
FOM (Power/ (Order×F_{cutoff}× SFDR×ENOB)) (fW/Hz)	0.090	-	0.122	-	0.165	0.175	0.164

3.5 Layout

Operational amplifier layout is shown in Figure 3.19. Layout size of the operational amplifier is 43.7 × 62.4 um^2.

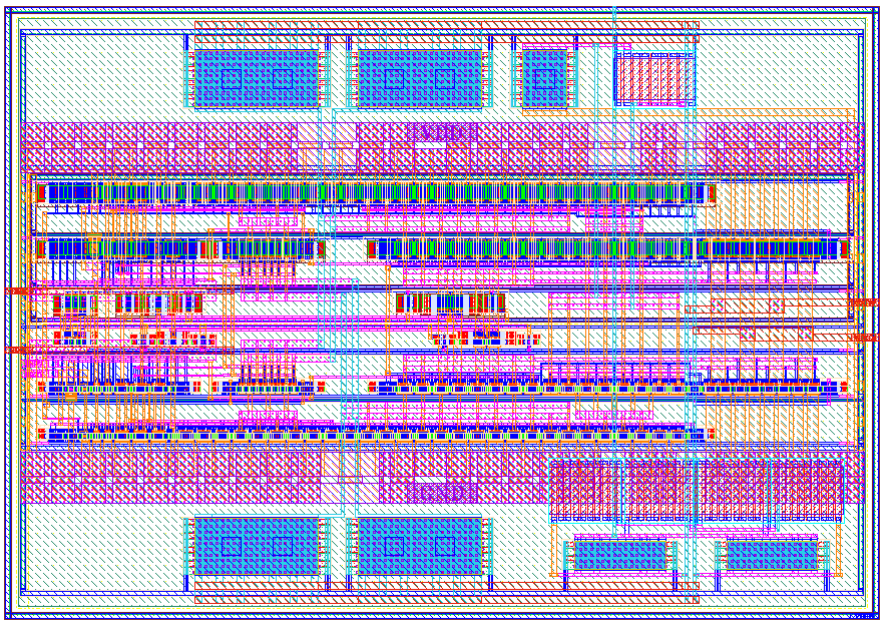

Figure 3.19 : Operational amplifier layout.

Layout of the filter is shown in Figure 3.20. Layout size of the 4^{th} order lowpass filter is 353.8×174.3 um^2 including the top-level power routings.

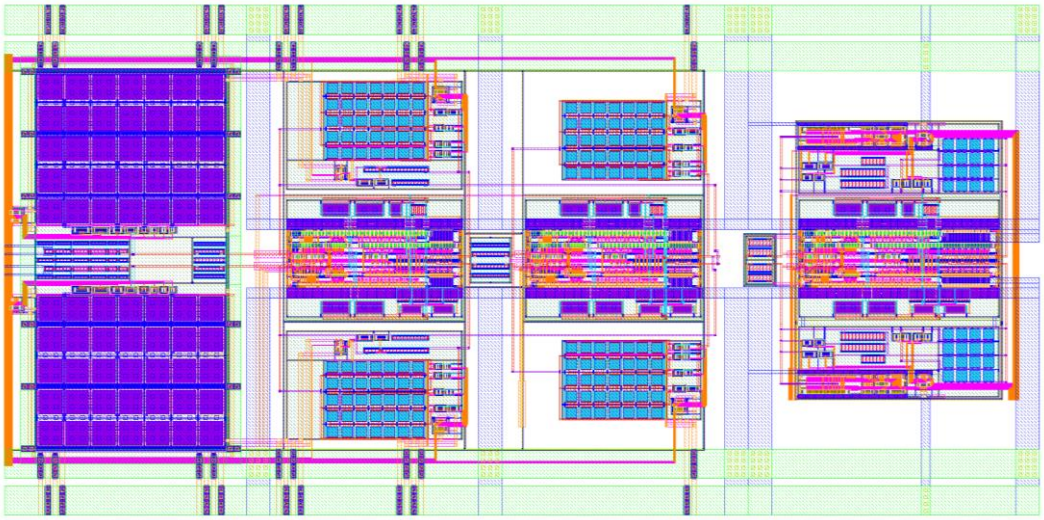

Figure 3.20 : 4^{th} order opamp-RC lowpass filter layout.

4. CONCLUSION

In the scope of this thesis, a fully differential opamp-RC lowpass filter is designed in 22 nm FDSOI process technology and simulated. Theory of the analog filter functions are studied. Most common circuit topologies used for implementation of lowpass filters are examined. Design and performance parameters of analog lowpass filters are explained in detail. FDSOI technology and its differences and advantages over bulk CMOS processes are explained. The design of the opamp-RC lowpass filter is explained in detail. Specifications and resulting design decisions are described. Schematics of the 3rd order Chebyshev type I lowpass filter and the variable gain first order filter, which are the subblocks the designed filter, are presented with detailed explanation. Schematics of the two-stage operational amplifier and the common mode feedback circuit are also presented with the design considerations. Additionally, designed switchable capacitor circuit and offset calibration circuit are demonstrated. Finally, simulation result of the designed operational amplifier and opamp-RC lowpass filter are illustrated and layout of the designed filter and operational amplifier are shown. Included DPD mode in the filter, for transforming the filter to a 0 dB gain buffer using the dedicated SPI bits when needed, is explained.

The circuit is designed in 22 nm FDSOI technology using flip-well MOSFET devices, MOM capacitors, polysilicon resistors and 0.8V supply voltage.

In conclusion, the designed opamp-RC lowpass filter has 60 dB stopband attenuation compared to the 12 dB passband gain and passband ripple less than 1dB. Passband and stopband corner frequencies are 25 MHz and 240 MHz respectively. 81 dB SFDR and 7.6 bits ENOB values are achieved for full scale input voltage.

REFERENCES

[1] **G. Dolmans et al.,** "UWB Radio Transceivers for Ultra Low Power and Low Data Rate Communications," 2007 IEEE International Conference on Ultra-Wideband, 2007, pp. 152-157, doi: 10.1109/ICUWB.2007.4380932.

[2] **A. Donno, S. D'Amico, M. De Matteis and A. Baschirotto,** "A 150MHz 3rd-order single Opamp continuous-time analog filter in 28nm CMOS technology," 2015 IEEE International Conference on Electronics, Circuits, and Systems (ICECS), 2015, pp. 161-164, doi: 10.1109/ICECS.2015.7440274.

[3] **M. Rachid, S. Pamarti and B. Daneshrad,** "Filtering by Aliasing," in IEEE Transactions on Signal Processing, vol. 61, no. 9, pp. 2319-2327, May1, 2013, doi: 10.1109/TSP.2013.2250971.

[4] **L. Ye, C. Shi, H. Liao, R. Huang and Y. Wang,** "Highly Power-Efficient Active-RC Filters with Wide Bandwidth-Range Using Low-Gain Push-Pull Opamps," in IEEE Transactions on Circuits and Systems I: Regular Papers, vol. 60, no. 1, pp. 95-107, Jan. 2013, doi: 10.1109/TCSI.2012.2215700.

[5] **L. Huelsman,** Active and passive analog filter design: An introduction. New York: McGraw-Hill, 1993.

[6] **A. Vasilopoulos, G. Vitzilaios, G. Theodoratos and Y. Papananos,** "A Low-Power Wideband Reconfigurable Integrated Active-RC Filter With 73 dB SFDR," in IEEE Journal of Solid-State Circuits, vol. 41, no. 9, pp. 1997-2008, Sept. 2006, doi: 10.1109/JSSC.2006.880616.

[7] **N. Planes et al.,** "28nm FDSOI technology platform for high-speed low-voltage digital applications," 2012 Symposium on VLSI Technology (VLSIT), 2012, pp. 133-134, doi: 10.1109/VLSIT.2012.6242497.

[8] **S. Makovejev, N. Planes,** et al., "Comparison of self-heating and its effect on analogue performance in 28 nm bulk and FDSOI," Solid-State Electronics, vol. 115, pp. 219–224, 2016.

[9] **V. Kilchytska et al.,** "Comparative study of non-linearities in 28 nm node FDSOI and Bulk MOSFETs," 2017 Joint International EUROSOI Workshop and International Conference on Ultimate Integration on Silicon (EUROSOI-ULIS), 2017, pp. 128-131, doi: 10.1109/ULIS.2017.7962581.

[10] **R. Schaumann, V. V. M. Elwyn, and H. Xiao,** Design of analog filters. New York u.a.: Oxford Univ. Press, 2010.

[11] **S.-B. Park,** "Compact High Performance Analog CMOS baseband design solutions for multistandard wireless transceivers," dissertation, Ohio State University, Columbus, OH, 2006.

[12] **H. Elwan, H. Alzaher and M. Ismail,** "A new generation of global wireless compatibility," in IEEE Circuits and Devices Magazine, vol. 17, no. 1, pp. 7-19, Jan. 2001, doi: 10.1109/101.900123.

[13] **H. G. Dimopoulos,** Analog Electronic Filters. Springer Netherlands, 2012.

[14] **E. Sackinger and W. Guggenbuhl,** "A versatile building block: the CMOS differential difference amplifier," in IEEE Journal of Solid-State Circuits, vol. 22, no. 2, pp. 287-294, April 1987, doi: 10.1109/JSSC.1987.1052715.

[15] **Steffes, M.** Design Methodology for MFB Filters in ADC Interface Applications (Application Report No. sboa114). 2006, Retrieved from Texas Instruments website: https://www.ti.com/lit/an/sboa114/sboa114.pdf

[16] **J. Mäkipää and O. Billoint,** "FDSOI versus BULK CMOS at 28 nm node which technology for ultra-low power design?," 2013 IEEE International Symposium on Circuits and Systems (ISCAS), 2013, pp. 554-557, doi: 10.1109/ISCAS.2013.6571903.

[17] **O. Weber,** "FDSOI vs FinFET: differentiating device features for ultra low power & IoT applications," 2017 IEEE International Conference on IC Design and Technology (ICICDT), 2017, pp. 1-3, doi: 10.1109/ICICDT.2017.7993513.

[18] **C. Mazuré, R. Ferrant, B. Nguyen, W. Schwarzenbach and C. Moulin,** "FDSOI: From substrate to devices and circuit applications," 2010 Proceedings of ESSCIRC, 2010, pp. 45-51, doi: 10.1109/ESSCIRC.2010.5619767.

[19] **S. Pavan and Y. Tsividis.** High Frequency Continuous Time Filters In Digital CMOS Processes. Kluwer Academic Publishers, Boston, 2000.

[20] **S.-J. Yoo,** "Design of analog baseband circuits for wireless communication receivers," dissertation, Ohio State University, Columbus, OH, 2004.

[21] **R. J. Baker,** CMOS mixed-signal circuit design. Hoboken, NJ: Wiley, 2009.

[22] **J. Ryynanen, M. Hotti, V. Saari,** et al., "WCDMA multicarrier receiver for base-station applications," Proceedings of the 31st European Solid-State Circuits Conference, 2005. ESSCIRC 2005.

[23] **S. D'Amico, V. Giannini, and A. Baschirotto,** "A 4th-order active gm-RC reconfigurable (UMTS/WLAN) filter," IEEE Journal of Solid-State Circuits, vol. 41, no. 7, pp. 1630–1637, 2006.

[24] **D. M. Monticelli,** "A quad CMOS single-supply op amp with rail-to-rail output swing," in IEEE Journal of Solid-State Circuits, vol. 21, no. 6, pp. 1026-1034, Dec. 1986, doi: 10.1109/JSSC.1986.1052645.

[25] **A. K. Gupta, V. Dhanasekaran,** et al., "Multipath common-mode feedback scheme suitable for high-frequency two-stage amplifiers," Electronics Letters, vol. 42, no. 9, p. 499, 2006.

[26] **H. Amir-Aslanzadeh, E. J. Pankratz and E. Sanchez-Sinencio,** "A 1-V +31 dBm IIP3, Reconfigurable, Continuously Tunable, Power-Adjustable Active-RC LPF," in IEEE Journal of Solid-State Circuits, vol. 44, no. 2, pp. 495-508, Feb. 2009, doi: 10.1109/JSSC.2008.2011037.

[27] **F. Lavalle-Aviles and E. Sánchez-Sinencio,** "A 0.6-V Power-Efficient Active-RC Analog Low-Pass Filter With Cutoff Frequency Selection," in IEEE Transactions on Very Large Scale Integration (VLSI) Systems, vol. 28, no. 8, pp. 1757-1769, Aug. 2020, doi: 10.1109/TVLSI.2020.2999414.

[28] **M. De Matteis, S. D'Amico and A. Baschirotto,** "A 0.55 V 60 dB-DR Fourth-Order Analog Baseband Filter," in IEEE Journal of Solid-State Circuits, vol. 44, no. 9, pp. 2525-2534, Sept. 2009, doi: 10.1109/JSSC.2009.2024801.

[29] **B. Vigraham, J. Kuppambatti and P. R. Kinget,** "Switched-Mode Operational Amplifiers and Their Application to Continuous-Time Filters in Nanoscale CMOS," in IEEE Journal of Solid-State Circuits, vol. 49, no. 12, pp. 2758-2772, Dec. 2014, doi: 10.1109/JSSC.2014.2354641.

[30] **Drost, M. Talegaonkar and P. K. Hanumolu,** "Analog Filter Design Using Ring Oscillator Integrators," in IEEE Journal of Solid-State Circuits, vol. 47, no. 12, pp. 3120-3129, Dec. 2012, doi: 10.1109/JSSC.2012.2225738.

CURRICULUM VITAE

Name Surname **:** Ömer Taha Keleş

Place and Date of Birth **:**

E-Mail **:**

EDUCATION **:**

- **B.Sc.** **:** 2018, Middle East Technical University